Proceedings of the 18th International Students Conference "Modern Analytical Chemistry"

Prague, 15—16 September 2022

Edited by Karel Nesměrák

FACULTY OF SCIENCE
Charles University

Prague 2022

Proceedings of the
18th International Students Conference
"Modern Analytical Chemistry"

Proceedings of the 18th International Students Conference "Modern Analytical Chemistry"

Prague, 15—16 September 2022

Edited by Karel Nesměrák

FACULTY OF SCIENCE
Charles University

Prague 2022

The electronic version of the Proceedings is available at the conference webpage:
http://www.natur.cuni.cz/isc-mac/

Preface

On September 15 and 16, 2022, young analytical chemists gathered in Prague for the 18th time to present their scientific achievements and share experiences. A total of 41 chemists, representing nine universities from six countries, had the opportunity to meet each other, have lively discussions, and exchange their ideas and accomplishments made in the fields of analytical chemistry. Additionally, participation in the conference further cultivated the presentation and language skills of the participants.

Twelve conference participants decided to publish the contributions that form these proceedings. Contributions are sorted by the delivery date and are supplemented by indexes, allowing navigation through the pages. The topics of the papers come from all three areas of instrumental analysis – electroanalytical, separation, and spectral methods – and show various applications for solving tasks for human society. Hopefully, the reader will find these contributions to be interesting, beneficial, and enjoyable reading.

The patronage of the Division of Analytical Chemistry of the European Chemical Society and the Working Group of Analytical Chemistry of the Czech Chemical Society are gratefully welcomed.

We are very grateful to all sponsors for their kind sponsorship making the conference possible but for their cooperation and support in many of our other activities.

doc. RNDr. Karel Nesměrák, Ph.D., *editor*

Sponsors

The organizers of 18th International Students Conference "Modern Analytical Chemistry" gratefully acknowledge the generous sponsorship of following companies:

www.analytika.net   www.thermofisher.cz   www.lach-ner.com

www.metrohm.com   nicoletcz.cz   www.optikinstruments.cz

www.2theta.cz   watrex.com   www.zentiva.cz

Contents

Evaluation of the stability of biologically active chlorinated arylcarbamoyl-naphthalenylcarbamates by RP-HPLC

Dominika Pindjaková[a, *], Marina Heceduš[a], Lucia Vráblová[a], Tomáš Goněc[b], Josef Jampílek[a]

[a] Department of Analytical Chemistry, Faculty of Natural Sciences, Comenius University, Ilkovičova 6, 842 15 Bratislava, Slovakia ✉ pindjakova.dominika@gmail.com

[b] Department of Chemical Drugs, Faculty of Pharmacy, Masaryk University, Palackého 1946/1, 612 00 Brno, Czech Republic

Keywords

carbamates

HPLC

phenyl-based stationary phases

stability

Abstract

The original carbamates with excellent antimicrobial activity derived from 1-hydroxy-*N*-(2,4,5-trichlorophenyl)-2-naphthamide were investigated for their stability. 2-[*N*-(2,4,5-Trichlorophenyl)-carbamoyl]naphthalen-1-yl ethyl carbamate with the weakest steric protection, i.e., with the expected highest degradability and two other carbamates with a more sterically protected carbamate bond (2-[*N*-(2,4,5-trichlorophenyl)carbamoyl]naphthalen-1-yl 2-phenyl-ethyl carbamate and 2-[*N*-(2,4,5-trichlorophenyl)carbamoyl]-naphthalen-1-yl isopropyl carbamate), i.e., with the expected lower degradability, were chosen. The developed HPLC methods using chromatographic columns with phenyl-based stationary phases and acetonitrile:phosphate buffer (pH = 2.5) as the mobile phases provided sufficient resolution between the studied carbamates and expected degradant, pattern anilide.

1. Introduction

Carbamates, derivatives of a hypothetical carbamic acid, are characterized by the presence of the –O–CO–NH– bond. This moiety is an important functional group that, due to its electronic properties, is able to interact and bind to a number of enzymes/receptors and elicit a biological response through these target sites. The properties of the carbamate moiety can be easily modified by various substitutions at the N– and O–termini. Carbamates are an integral part of many drugs and prodrugs approved by the US Food and Drug Administration and the European Medicines Agency. Many compounds that contain a carbamate group are currently in various stages of preclinical and clinical trials [1, 2].

The stability of a drug is its resistance to chemical, physical, and micro-biological effects that could alter its initial physicochemical properties during transport, storage, and use [3, 4]. Drugs are not infinitely fixed systems. Insufficient stability of drugs can result in loss of activity, decreased concentration of active substance, increased concentration of toxic products, change in bioavailability, or loss of system integrity. The criterion for pharmaceutical stability of drugs is the assessment of the impact of various environmental factors on the quality of the medicinal product and thus on the suitability of its use in therapy. Therefore, for the purpose of testing the stability of medicinal products, it is necessary to determine the shelf-life of the medicinal product and to specify the storage conditions under which the medicinal product remains stable and does not lose more than 5% of the active substance.

Stability testing requires the use of an appropriately selected analytical method that is able to monitor the substance content without interfering with decomposition products and other impurities. Any approach to their evaluation should be comprehensive, simple, and easy to implement. One of these approaches may be reversed-phase high performance liquid chromatography (RP-HPLC), which is the most commonly used analytical separation technique [5].

A study on antistaphylococcal activities and ADME-related properties of new chlorinated arylcarbamoylnaphthalenylcarbamates was recently published [6]. Since carbamates are a relatively unstable part of the molecule [7], based on different substitutions of the carbamate moiety providing different steric protection, three molecules were chosen for experimental determination of their stability under conditions that simulate biological tests. The aim of this paper is to present the development of the analytical method and the stability results obtained.

2. Experimental

2.1 Instrumentation

A HPLC separation module Agilent 1200 Series (Agilent Technologies, USA) equipped with a Dual Absorbance Detector (DAD SL G1315C, Agilent Technologies) was used to evaluate carbamate stability. A chromatographic column XTerra® Phenyl (100×4.6 mm, 3.5 μm; Waters, USA) for the evaluation of the compounds NM-58a and NM-58h and a chromatographic column Luna® Phenyl-Hexyl (250×4.6 mm, 5 μm; Phenomenex, USA) for the evaluation of the compound NM-58o were used. The HPLC separation process was monitored by ChemStation for LC 3D systems (Agilent Technologies). Isocratic elution by mixtures of acetonitrile (HPLC grade), 60% for NM-58a and NM-58h, 70% for NM-58o, and phosphate buffer (pH= 2.5), 40% for NM-58a and NM-58h, 30% for NM-58o, as mobile phases was used. The total flow of the column was 1.0 mL min^{-1}, injection 20 μL, column temperature 40 °C, sample temperature 10 °C, the time of analysis

was 15 and 8 min, respectively. The detection wavelength of 254 nm was chosen. The retention time of carbamate NM-58a was 4.92±0.05 min, carbamate NM-58h was 3.57±0.05 min, and anilide NM-58 was 3.08±0.05 min. When the method using the Luna® Phenyl-Hexyl column was applied, the retention time of carbamate NM-58o was 9.78±0.05 min and anilide NM-58 was 13.59±0.05 min. The limit of detection of anilide NM-58 on the XTerra® Phenyl column was 8.5 ng mL^{-1} and the limit od fetection of anilide on the Luna® Phenyl-Hexyl column was 10.5 ng mL^{-1}.

2.2. Sample preparation

Approximately 2 mg of selected carbamate were weighed into 25 mL Erlenmeyer flasks and dissolved in phosphate buffers with pH = 6, 7 and 8. For compounds NM-58h and NM-58o were used only phosphate buffers with pH = 7 and 8, because the samples are more stable in an acidic environment than in a neutral and alkaline environment. The flasks were coated with parafilm. The prepared samples were stirred at 37 °C in a water bath for 3 days, fractions were taken at time intervals (0.0, 0.5, 1.0, 1.5, 2.0, 2.5, 3.0, 4.0, 5.0, 6.0, 12, 24, 48, and 72 h) and injected into the HPLC system. Each experiment was repeated three times. Each sample was analyzed twice.

3. Results and discussion

From the prepared series of thirteen chlorinated arylcarbamoylnaphthalenyl-carbamates, three derivatives were selected to determine the stability. Ethyl carbamate NM-58a was selected for stability evaluation as the derivative with the expected lowest stability due to the least steric protection of the carbamate bond. Phenylethyl carbamate NM-58o represents derivatives with a longer chain, i.e., with the assumed higher stability, and isopropyl carbamate NM-58h is a derivative with branching at the α-carbon, i.e., with the expected highest stability due to the steric protection of the carbamate bond (Fig. 1). For the three compounds, the parent anilide NM-58 was formed as a degradation product (Fig. 1).

Because the investigated compounds are rather planar and consist of aromatic nuclei, the type of phenyl column was chosen, namely XTerra® Phenyl. Based on previous experience, a mixture of acetonitrile and phosphate buffer pH = 2.5 was tested as the mobile phase and an acetonitrile:buffer ratio of 60:40 (*v/v*) for ethyl NM-58a and isopropyl NM-58h carbamates was chosen due to good peak resolution and appropriate time analysis. Figures 2a and 2b show chromatograms of spiked mixtures of parent anilide and test substances NM-58a and NM-58h.
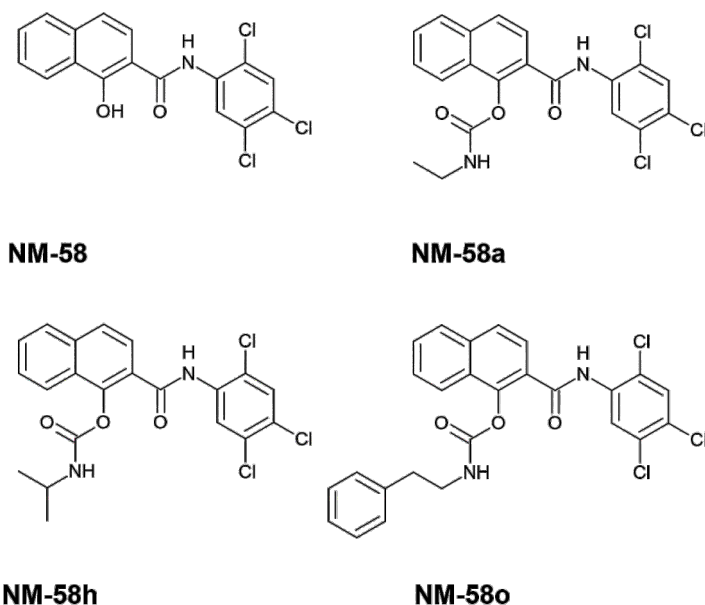
Fig. 1 Three evaluated arylcarbamoylnaphthalenylcarbamates (NM-58a, NM-58h, and NM-58o) and pattern anilide (NM-58).

However, the conditions described above proved to be unsuitable for the mixture of anilide NM-58 and phenylethyl carbamate NM-58o, because the retention times of both analytes were only slightly different, which manifested itself as a peak overlap. None of the modifications of the analysis conditions (including the change in the composition or the ratio of the mobile phase components) achieved the desired separation. The retention times of both compounds only shifted, but the overlap of the peaks was maintained.

Thus, the column was changed, and Luna® Phenyl-Hexyl being selected as the chromatographic column with a suitable stationary phase. Again, different ratios of acetonitrile and buffer were tested, and acetonitrile:phosphate buffer pH = 2.5 with a ratio of 70:30 (*v/v*) was chosen as the most optimal mobile phase. The retention times of the spiked sample of analytes NM-58 and NM-58o are shown in the chromatogram in Fig. 2c.

The decomposition process of carbamates NM-58a (at pH = 6, 7 and 8), NM-58h (at pH = 7 and 8) and NM-58o (at pH = 7 and 8) can be described by pseudo-first order kinetics. The calculated values of decomposition (reaction) rate and half-life are given in Table 1 and were calculated from the slope of the graphs of the natural logarithm of the residual reactant fraction as a function of time by statistical regression analysis. Table 1 shows that the ethyl derivative NM-58a at alkaline pH = 8 has a $\tau_{0.5}$ of approximately 9 days, while already at neutral pH the $\tau_{0.5}$ is approximately 23 days. As for isopropyl carbamate NM-58h, it can be stated that the half-life at neutral pH is approximately 88 days and at alkaline pH it has been 13 days. Phenylethyl carbamate NM-58o is stable at neutral pH with a half-life of
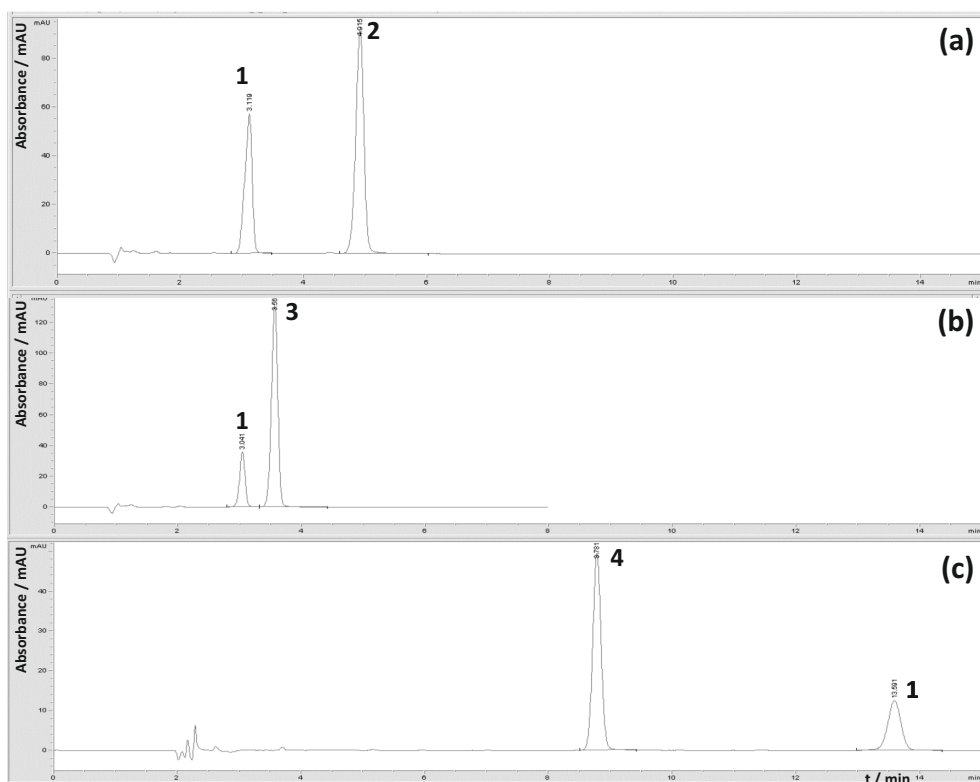
Fig. 2 Chromatograms of separated mixtures of parent anilide and selected carbamates (a, b) on XTerra® Phenyl column using acetonitrile:phosphate buffer (pH = 2.5) 60:40 (*v/v*), compounds (1) NM-58, (2) NM-58a, (3) NM-58h; (c) on Luna® Phenyl-Hexyl column using acetonitrile:phosphate buffer (pH = 2.5) 70:30 (*v/v*), compounds (4) NM-58o, (1) NM-58.

Table 1
Calculated values of the rate constant and half-life of the substances studied.

Compound	pH	$k / \mathrm{h^{-1}}$	$\tau_{0.5} / \mathrm{h}$
NM-58a	6	$5.77 \cdot 10^{-4}$	1201.8
	7	$1.25 \cdot 10^{-3}$	555.8
	8	$3.17 \cdot 10^{-3}$	218.8
NM-58h	7	$3.28 \cdot 10^{-4}$	2112.1
	8	$2.09 \cdot 10^{-3}$	331.5
NM-58o	7	$9.67 \cdot 10^{-4}$	716.4
	8	$2.04 \cdot 10^{-3}$	339.3

approximately 29 days and at alkaline pH the value is 14 days. Since biological experiments are performed in media with a pH range of 6–7 and a maximum of 48 hours, it can be stated that the compounds are stable enough to be tested for biological activity.

4. Conclusions

In this study, RP-HPLC methods were developed to evaluate the stability of three biologically active chlorinated arylcarbamoylnaphthalenylcarbamates selected on the basis of the different steric protection of the carbamate group. Compound NM-58a contained a less sterically protected carbamate group compared to derivatives NM-58h and NM-58o. Chromatographic columns with phenyl-based stationary phases and mixtures of acetonitrile and phosphate buffer pH = 2.5 were used to separate the carbamates and their degradant. The results obtained indicate that these three analyzed agents are stable enough to be tested for biological activity under acidic and/or neutral pH conditions. However, in alkaline conditions, their stability is significantly shortened.

References

[1]   Ghosh A.K., Brindisi M.: Urea derivatives in modern drug discovery and medicinal chemistry. *Journal of Medicinal Chemistry* **63** (2020), 2751–2788.
[2]   Adams P., Baron, F.A.: Esters of carbamic acid. *Chemical Reviews* **65** (1965), 567–602.
[3]   Carstensen J.T.: *Drug Stability: Principles and Practices.* Marcel Dekker, New York 1990.
[4]   Huynh-Ba K.: *Handbook of Stability Testing in Pharmaceutical Development.* Springer, New York 2009.
[5]   Sarker S. D., Nahar L.: Applications of High Performance Liquid Chromatography in the Analysis of Herbal Products. In: *Evidence-Based Validation of Herbal Medicine*. P.K. Muk-herjee (ed.). Elsevier 2015, p. 405–425.
[6]   Gonec T., Pindjakova D., Vrablova L., Strharsky T., Michnova H., Kauerova T., Kollar P., Oravec M., Jendrzejewska I., Cizek A., Jampilek J.: Antistaphylococcal activities and ADME-related properties of chlorinated arylcarbamoylnaphthalenylcarbamates. *Pharmaceuticals* **15** (2022), 715.
[7]   Karaman R.: Prodrugs design based on inter- and intramolecular chemical processes. *Chemical Biology and Drug Design* **82** (2013), 643–668.

HPLC method development for untargeted metabolomics of polar compounds

Anna Jelínková[a, b, *], Tommaso Stefani[c], Zdeněk Kameník[c], Anna Kubíčková[a]

[a] *Department of Analytical Chemistry, Faculty of Science, Charles University,
   Hlavova 2030/8, 128 43 Prague 2, Czech Republic ✉ jelinkova@natur.cuni.cz*
[b] *Laboratory of Gnotobiology, Institute of Microbiology of the Czech Academy of Sciences,
   Doly 183, 549 22 Nový Hrádek, Czech Republic*
[b] *Laboratory for the Biology of Secondary Metabolism Institute of Microbiology of the Czech
   Academy of Sciences, Vídeňská 1083, 142 20 Prague 4, Czech Republic*

Keywords
HILIC
LC-MS metabolomics
polar metabolites

Abstract
LC-MS-based metabolomics is a fast-spreading approach to study microorganisms and their metabolism. This work is focused on LC-MS metabolomics of polar compounds, which are not retained on chromatographic columns using the well-established reversed-phase mechanism. The HILIC and multimode columns are expected to improve the retention characteristics of polar compounds. In the experimental part, four HILIC columns and two mixed-mode columns were tested. The columns were compared with a CSH-C18 column, using a set of 258 polar, human and microbial metabolites with a high diversity of their physicochemical properties. All HILIC columns significantly extended the range of the CSH-C18 column. In terms of the number of compounds detected, the BEH Amide PEEK column using ammonium acetate pH = 3 had the highest ability to analyze a wide spectrum of polar metabolites. The combination of the mentioned results is promising for the use of this method in untargeted metabolomics.

1. Introduction

Metabolomics is an omics approach focusing on small molecules (max. 1 500 Da) within a biological sample (cell, tissue, whole organism) [1]. Such studies offer reflection of an organism actual status, both in health and disease. Metabolite profiles can describe microbiota composition in gut microbiota-related research and lead to the discovery of biomarkers, important in the development of methods for nutritional and personalized therapies [2]. According to the detected compounds, metabolomics approaches can be divided into two groups: targeted metabolomics, focusing on analysis of small group of homogenous metabolites, and untargeted metabolomics, focused on analysis of all metabolites within the sample [3]. In addition, untargeted metabolomics can supplement information obtained from genomics or transcriptomics analysis. In contrast with these

mentioned omics approaches studying sets of very similar compounds, metabolomics studies heterogenous set of compounds differing in their physical-chemical properties, which causing main challenges in analytical methods using untargeted metabolomics [4].

One of the widely used analytical method employed in metabolomics is liquid chromatography-mass spectrometry (LC-MS). Main benefits of this method are high sensitivity, easy sample preparation and high variety of columns which could be used. The most usual and well-established system is RP-LC system employing C18 columns. However, this system does not enable detection of polar compounds, which are involved in a multitude of important biological processes. As an alternative, hydrophilic interaction liquid chromatography (HILIC) can be used to overcome this limitation and amplify working range of C18 [5]. HILIC employ conditions suitable mainly for the analysis of polar, hydrophilic substances such as amino acids, nucleosides, organic acids or sugars, which are typical representatives of metabolome [1, 5].

The aim of this study was to analyze the same set of 258 compounds using HILIC, multimode columns and C18 column as a reference, process the results and compare them in terms of maximal number of detected standards and ability to widened the range of analyzable compounds of CSH-C18.

2. Experimental

2.1 Reagents and chemicals

Analytes: 258 chemical individuals, standards of common metabolites varying in polarities, simulating variety of real metabolome (highest molar mass: 767.091 Da -NADPH)

Solvents and buffers: acetonitrile (Biosolve), methanol, ammonia 32%, formic acid 99%, acetic acid (VWR Chemicals), medronic acid (Agilent), MiliQ Water (LC Pack Millipore), phosphoric acid (Sigma). All solvents were used in LC-MS grade.

2.2 Samples preparation

In total 258 chemicals including characteristic compounds contained in eukaryotic and prokaryotic metabolomes were weighted and diluted with MiliQ water to the concentration of 1 mg/mL. Samples were pooled into 8 mixtures to the final concentration 30 μg/mL of each compound. Composition of pooled samples was chosen based on the masses of compounds to prevent m/z duplicity within one pooled sample. Finally, mixture was diluted with acetonitrile 1:1, medronic acid in concentration 5 μM was added to each pooled sample and samples were stored in −20 °C freezer until their analysis.

Table 1
Specification of chromatography columns used for experimental work.

Column name	Producer	Length, diameter, particle size	Type of chromato-graphy, ligand
BEH Amide PEEK	Waters, USA	100×2.1 mm; 1.7µm	HILIC, amide
Infinity Lab Poroshell 120 HILIC-Z	Agilent, USA	100×2.1 mm; 2.7µm	HILIC, sulfobetain
ZIC-HILIC	SeQuant, Germany	100×2.1 mm; 3.5µm	HILIC, zwitteriont
Triart Diol-HILIC	YMC, Japan	100×2.1 mm; 1.9 µm	HILIC, dihydroxypropyl
Scherzo SS-C18	Imtact, Japan	100×3 mm; 3 µm	Multimode
Atlantis	Waters, USA	100×2.1 mm; 1.7µm	Multimode
CSH-C18	Waters, USA	100×2.1 mm; 1.7µm	RP-chromatography, C18

Table 2
Mobile phases and gradients used for HILIC columns, multimode columns and CSH-C18 column.

	HILIC columns		Multimode columns	CSH-C18
Mobile phase A	18 mM ammonium formate in 40% acetonitrile	18 mM ammonium acetate in 40% acetonitrile	0.1% formic acid	0.1% formic acid
Mobile phase B	5 mM ammonium formate in 95% acetonitrile	5 mM ammonium acetate in 95% acetonitrile	100 mM ammonium acetate	acetonitrile
Mobile phase C	n/a	n/a	acetonitrile	n/a
pH	3.0; 9.0	5.8	5.8	n/a
	Time [min]/%A–B		Time [min]/%A–B–C	Time [min]/%A–B
Linear gradient	0/0–100		0/100–0–0	0/95–5
	0.5/0–100		1/100–0–0	1/95–5
	12.5/100–0		9.5/0–40–60	12.5/0–100
	12.6/0–100		12.5/0–0–100	13/0–100
	14/0–100		13/0–0–100	13.1/95–5
	–		13.1/100–0–0	14/95–5
	–		14/100–0–0	–

2.3 LC-MS Instrumentation

Seven chromatography columns were used in this comparative study-four HILIC columns (BEH Amide PEEK, Diol-HILIC, ZIC-HILIC, HILIC-Z), two multimodal columns (Atlantis, Scherzo SS-C18) and CSH-C18 column. Detailed parameters of chromatography columns used in this study are listed in Table 1. Each column was passivated overnight prior to the analysis using acetonitrile and 0.5% H_3PO_4 in MiliQ water 1:1. Also, same procedure was done for 15 minutes before the analysis with 0.5% H_3PO_4 in MiliQ water with flow 1 mL/min. After washing and conditioning of the columns, 1 µL of each pooled sample was analyzed using gradient elution. Mobile phases and used gradients are listed in Table 2.
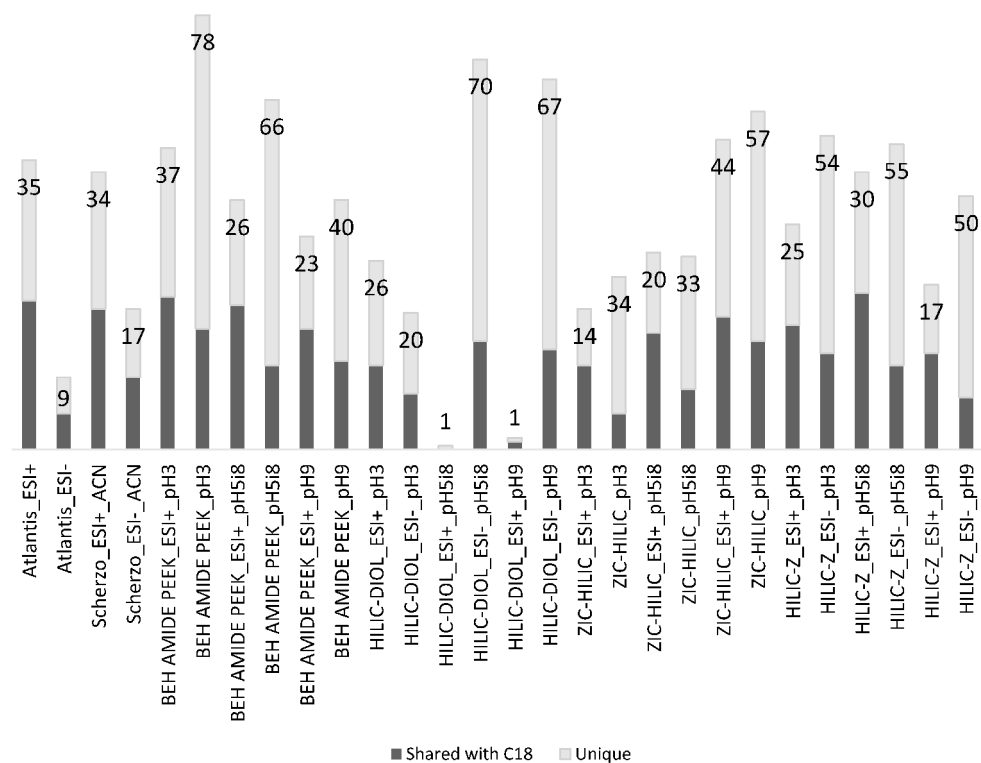
Fig. 1 Column graphs showing numbers of shared and unique (not dected on CSH-C18) standards, which are detected by each column and condition, in comparison with CSH-C18 column.

Samples were analyzed using 6576 LC/Q-TOF (Agilent Technologies, USA) coupled with 1290 Infinity II LC system. Instrument was consisted of Agilent 1290 Infinity II pump (G7120A), autosampler with thermostat (Vialsampler with thermostat G7129B), thermostat (Multicolumn thermostat G7116B) and mass spectrometer 6546 LC/Q-TOF. ESI Agilent Jet Stream technology was used as an ion source. Mass spectrometer was consisted of one quadrupole and time-of-flight analyzer equipped with reflectone for high resolution. Mass spectrometer switched between both negative and positive mode. Nitrogen was used as a dissolving gas. Scan speed was set for 4 scans/second and masses were measured in range of 50–1000 m/z. Reference masses were set as 112.050873 Da and 922.009798 Da to ensure correct measuring. Obtained data were analyzed using Agilent MassHunter software.

3. Results and discussion

After the data processing, we checked an ability of HILIC columns to increase the number of detected compounds in compare with CSH-C18. Results are shown as a column graph (Fig. 1), illustrating unique compounds detected exclusively by

Table 3

Division of analyzed standards into groups based on their structure.

Name of the group	Number of compounds
Aminoacids	70
Sacharides	23
Phosphorylated compounds	31
Beta-lactame antimicrobials	5
Bile acids	7
Catecholamines	8
Alcohols and aldehydes	5
Amines	32
Sulphur atom containing compounds	24
Purines and pyrimidines	15
Carboxylic acids	37
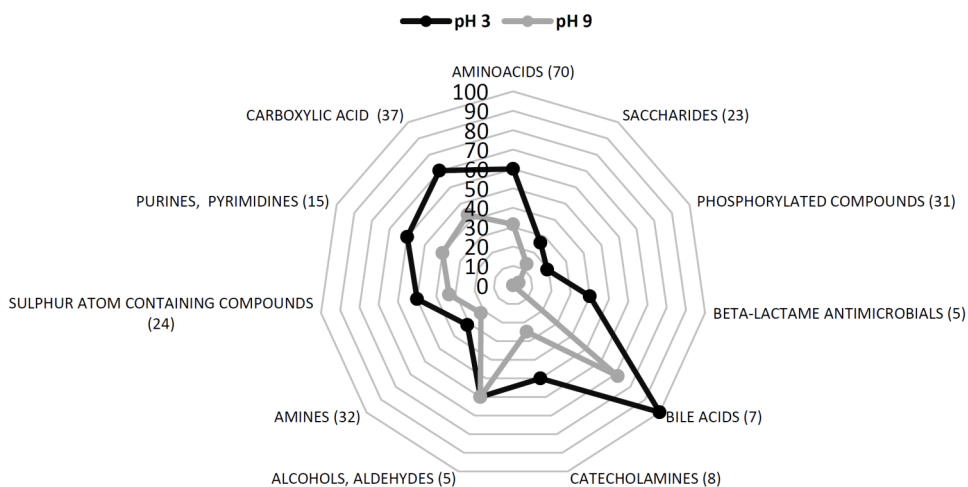
Fig. 2 Ray graph showing percentage of detected compounds in individual groups of standards using BEH Amide PEEK column in negative MS mode.

particular HILIC or multimode column, and amount of compounds detected by both compared systems. From the results, we can confirm that both HILIC and multimode columns extend the working range of RP system represented by CSH-C18 chromatography column and enable to spread coverage of detected compounds significantly. In addition, based on this graph we can compare the columns in terms of number of detected standards. Maximal amount of compounds was successfully detected using BEH Amide PEEK column using mobile phase pH = 3 ammonium formate buffer in acetonitrile and negative mode of the mass detector (Fig. 1).

For the visualization of results for individual columns, analyzed compounds were divided into groups based on the functional group present in their structure, as described in Table 3. The amount of detected compounds was visualized using ray graphs, which enable to show the percentage of detected standards in each

group. Graphs were generated separately for a given chromatographic column and mass detector mode.

As we can see from the ray graph showing results of BEH Amide PEEK column in ESI-mode (Fig. 2), we were able to detect majority of acids – bile acids, aminoacids or carboxylic acid group – whereas group of saccharides and phos-phates are not detected. However, these groups of compounds were critical and their limited detection was the case for other columns and conditions as well. Above all, good behavior of HILIC columns containing amide ligand in stationary phase is also described in literature, in studies for both targeted [7] and untargeted [8] metabolomics.

4. Conclusions

From our results, we conclude that HILIC and multimode columns enhance C18 column range for polar compounds detection. We confirmed that column is an essential part of chromatographic system and stationary phase is key parameter influencing ability to detect compounds. Based on our observations, methods using HILIC and multimode columns have a high potential to be employed in untargeted metabolomics of real samples, e.g., urine, plasma or feces.

References

[1]   Zhou B., Xiao J. F., Tuli L., Ressom H. W.: LC-MS-based metabolomics. *Molecular BioSystems* **8** (2012), 470–481.
[2]   Beger R., Dunn W., Schmidt M., Gross S., Kirwan J., Cascante M., Brennan L., Wishart D., Oresic M., Hankemeier T., Broadhurst D., Lane A., Suhre K., Kastenmüller G., Sumner S., Thiele I., Fiehn O., Kaddurah-Daouk R.: Metabolomics enables precision medicine: "A White Paper, Community Perspective". *An Official Journal of the Metabolomics Society* **12** (2016), 1–15.
[3]   Villas-Bôas S. G., Mas S., Åkesson M., Smedsgaard J., Nielsen J.: Mass spectrometry in metabolome analysis. *Mass Spectrometry Reviews* **24** (2005), 613–646.
[4]   Haggarty J., Burgess K. E. V.: Recent advances in liquid and gas chromatography methodology for extending coverage of the metabolome. *Current Opinion in Biotechnology* **43** (2017), 77–85.
[5]   Buszewski B., Noga S.: Hydrophilic interaction liquid chromatography (HILIC)—a powerful separation technique. *Analytical and Bioanalytical Chemistry* **402** (2012), 231–247.
[6]   Contrepois K., Jiang L., Snyder M.: Optimized analytical procedures for the untargeted metabolomic profiling of human urine and plasma by combining hydrophilic interaction (HILIC) and reverse-phase liquid chromatography (RPLC)-mass spectrometry. *Molecular & Cellular Proteomics* **14** (2015), 1684–1695.
[7]   Nelis M., Decraecker L., Boeckxstaens G., Augustijns P., Cabooter D.: Development of a HILIC-MS/MS method for the quantification of histamine and its main metabolites in human urine samples. *Talanta* **220** (2020), 121328.
[8]   Virgiliou C., Sampsonidis I., Gika H. G., Raikos N., Theodoridis G. A.: Development and validation of a HILIC-MS/MS multitarget method for metabolomics applications. *Electrophoresis* **36** (2015), 2215–2225.

Interfacing mass spectrometry with electrochemistry in the field of industrial battery research

Janik Scharf[a, *], Frank-Michael Matysik[b]

[a]   *BMW Group, Battery Cell Competence Center, 808 09 Munich, Germany* ✉ *Janik.Scharf@bmw.de*
[b]   *Institute of Analytical Chemistry, Chemo- and Biosensors, University of Regensburg,*
    930 53 Regensburg, Germany

Keywords

batteries
background
    determination
gas analysis
lithium-ion battery
mass spectrometry
response time

Abstract

The combination of mass spectrometry and electrochemistry to so-called Online Electrochemical Mass Spectrometry (OEMS) has been proofed as a powerful analytical technique to investigate Lithium-Ion Battery Cells during operation as it allows a time and potential resolved view onto the evolving gasses under quantitative and qualitative aspects. Herein, we describe the benefits of this new analytical technique in the use of the industrial battery research. Furthermore, the first steps by setting-up this kind of instrument, e. g., retention time and response characteristics as well as background determination are described in more detail.

1. Introduction

Lithium-Ion Batteries (LIBs) have become an integral part of our daily life. Within recent years, the usage has grown significantly, mainly by the demand for Electric Vehicles as well as other application purposes, e. g., Smart- & Headphones [1, 2]. However, the lifetime of a LIB is naturally determined by the extent of side reactions, fading an irreversible capacity loss, impedance increase, gas evolution and cell swelling. In order to use the full potential of future LIBs their ageing and the resulting consequences must be understood in more detail. Therefore, new advanced analytical measurement techniques with high selectivity and sensitivity are needed. A sophisticated approach is the combination of electrochemical experiments with *in-operando* measurements. One of the most widely used analytical techniques is mass spectrometry, as it can be easily interfaced to neighboring analytical and electrochemical techniques [1, 3, 4]

In this report, a detailed description of a measurement technique, so-called Online-Electrochemical Mass Spectrometry (OEMS) is introduced. As each setup strongly depends on the custom used instrument and parts, reaching from the
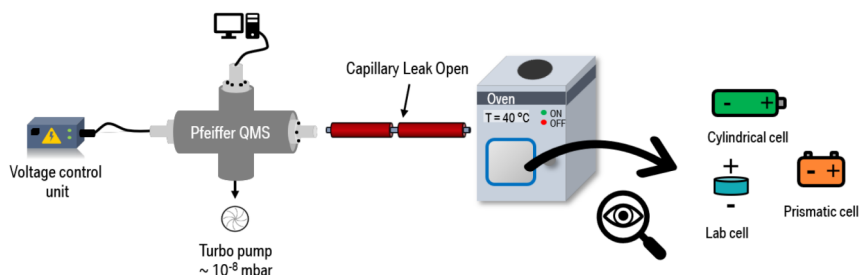
Fig. 1 Scheme of the used OEMS-Setup. The main parts are the Highquad mass spectrometer from Pfeiffer Vacuum, the crimped capillary from VTI and the climate-temperature system from CTS. The battery cells are cycled by using a Biologic VSP300 potentiostat.
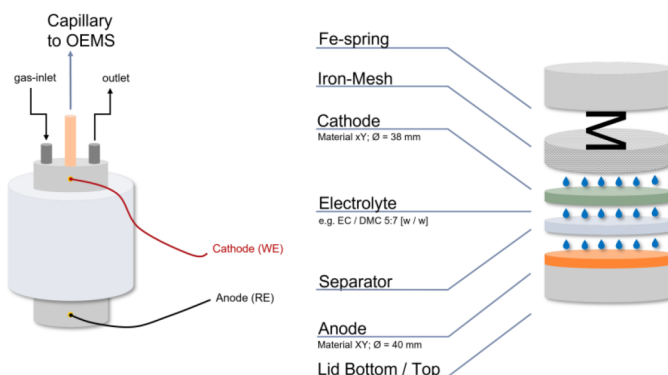
Fig. 2 Schematic lab cell setup for one compartment OEMS lab cells. The cell consists of an anode and cathode sheet, which were isolated from each by a separator, soaked with electrolyte. The lid and bottom / top seals the cell airtight. The iron mesh allows an easier separation of the gases.

used hardware up to the interface between mass spectrometry and electro-chemical cell, there is usually a resulting lack of information about the first steps.

2. Experimental

2.1 Setup

For mass detection a HiQuad QMA410 cross-beam mass spectrometer with a continuous secondary electron multiplier detector was used. The working pressure in the ionization chamber was kept at 10^{-7} mbar during measurement by using a turbomolecular pump (HiCube300, Pfeiffer Vacuum). To perform tests under specific conditions the electrochemical cell is integrated inside a temperature controlled oven (CTS, Type: T-40/25/S), Fig. 1. For electrochemical investigations a BioLogic potentiostat is used. The electrochemical cell body is made out of Kel-F, Fig. 2. The cell bottom as well as cell lid are made out of stainless

steel. The cell lid has three connections pipes, made out of Swagelok screw connectors. Two are used as gas inlet and outlet (to flush the cell with calibration gas or inert gas) and the third one is used to connect the cell via a crimped capillary (Vacuum Technology Incorporation) directly to the mass spectrometer.

2.2 Materials

$LiPF_6$ (1-M, CapChem) diluted in ethylene carbonate and ethyl methyl carbonate (3:7, *w/w*) was used as electrolyte. For response time evaluation a 1-M Na_2SO_4 (Merck Group) solution was used. For all experiments the cell parts were dried under vacuum and transferred in a glove box. After assembling the cell was transferred again from the glove box to the OEMS setup and were directly connected via the swagelok capillary connectors. For the background determination (Section 3.2) the cell parts were assembled, after 200 µL of electrolyte were injected into the electrochemical cell.

3. Results and discussion

3.1 Evaluation of the response time

The response time is the time, it takes for gaseous products to reach the detector in the MS and is therefore an important measure for each individual setup. So far, in many setups only the theoretical time, based on the diffusion length from the cell headspace to the MS is roughly estimated and can vary from several seconds up to minutes. The ambitious reader is referred to [1, 5, 6]. All response time scales are justified in order, that the measurement usually takes place for hours up to days. However, from an analytical perspective the response time should be determined, as the time which is required from an induced electrochemical impulse, which triggers a decomposition with gaseous products [6]. In our case, the electro-chemical decomposition of water was chosen as a model decomposition reaction. In order to catalyze the water splitting reaction, a solution of 1M Na_2SO_4 was used and the H_2 and O_2 evolution was monitored by applying a potential of approx. 3 V, shown in Fig. 3. From there it can be seen, that the response time is estimated within 5 minutes between electrochemical signal impulse and a change in the ion current. A maximum of the hydrogen and oxygen signal is achieved after 20 minutes before the signals are decreasing again.

3.2 Background determination

As this setup is used to detect minor side reaction, all disturbing mass-traces during the measurement have to be removed from further measurements. The evaporating electrolyte contributes considerably to the background noise. Therefore, a measurement of pure electrolyte has to be performed. Besides this
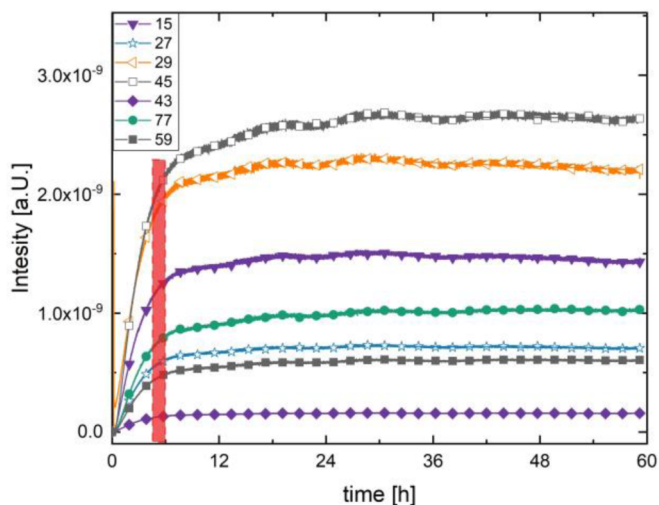
Fig. 4 Background determination of the mass traces (m/z ratios) with the strongest contribution of the used electrolyte. The equilibrium time (red rectangle) is determined to be 5 h after connecting the cell. The fluctuation in the mass channels are due to minor changes in pressure and temperature during the measurement.
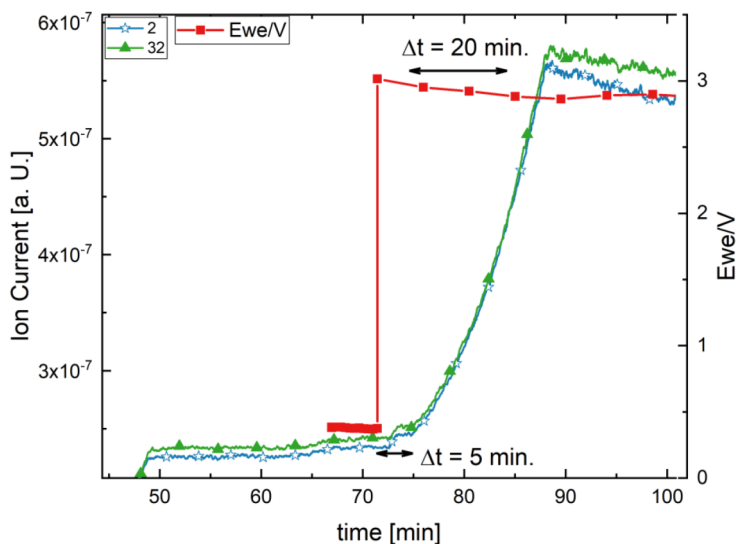
Fig. 3 Response time determination of the used setup, by using the electrochemical water splitting reaction. After applying a voltage of 3 V (red-square dotted), the mass traces of hydrogen ($m/z = 2$, blue stars) and oxygen ($m/z = 32$, green triangles) are rising within 5 minutes and the maximum of the signals were achieved after roughly 20 minutes.

background determination, the equilibration time of the setup can be evaluated. This is the time, which is required until all mass traces, related to the electrolyte are at a constant plateau. As the cell is assembled under glove box conditions, the headspace contains firstly only argon and is slowly replaced by the evaporating electrolyte. The electrochemical experiment should be only started, when the mass traces of the electrolyte induced background is at an sufficient stable plateau, therefore it is necessary to know the evaporation behavior of the electrolyte as well as the background noise, due to minor leakages. The value is specific for every setup and has to be determined every time by changing the setup or using different electrolyte compositions. As it can be seen in Fig. 4, the exemplarily depicted mass traces (m/z values) with the highest contribution are rising after connecting the cell to the setup (t = 0) equally, until they reach a plateau at a recent point. The equilibration time was determined to be five hours in our setup. Typical equilibration times, which were found in literature, are between four and six hours [6]. As the typical time of battery cycling experiments is far longer (up to days and weeks) this estimation is justified. Moreover it only means that a connected cell should rest for at least five hours until the stressful cycling procedure starts. The final background values can be read out of this experiment by fitting on an appropriate amount of time, in this case the last twenty hours.

4. Conclusion

In summary, a detailed description of our used OEMS setup as well as the fundamental characteristics, such as response and background factors have been presented. The response time was evaluated by using the electrochemical water splitting reactions and the background noise was determined by using pure electrolyte, from where it was also possible to determine the equilibration time. Despite that, the instrument is still in an optimization progress and further investigations on these factors has to be performed from time to time and has to be compared to the here presented very rudimentary values and how they can be improved, e.g., by using an optimized lab cell with a closer interface between cell and MS and an optimized galvanostatic cycling procedure for example a pulsed amperometric current sequence for the detection of the response time. Nevertheless, these values were determined for the first time on this setup and are showing a behavior of the overall setup to be ready for the use of LIB-cycling investigations.

References

[1]   He M., Castel E., Laumann A., Nuspl G., Novák P., Berg E.: In situ gas analysis of $Li_4Ti_5O_{12}$ based electrodes at elevated temperatures. *Journal of The Electrochemical Society* **162** (2015), A870–A876.

[2]   Etacheri V., Marom R., Elazari R., Salitra G., Aurbach D.: Challenges in the development of advanced Li-ion batteries: A review. *Energy & Environmental Science* **4** (2011), 3243–3262.

[3]   Lundström R., Berg E.: Design and validation of an online partial and total pressure measurement system for Li-ion cells. *Journal of Power Sources* **485** (2021), 229347.

[4]   Tsiouvaras N., Meini S., Buchberger I., Gasteiger H. A.: A novel on-line mass spectrometer design for the study of multiple charging cycles of a $Li-O_2$ battery. *Journal of The Electrochemical Society* **160** (2013), A471–A477.

[5]   Mattinen U., Klett M., Lindbergh G., Wreland Lindström R.: Gas evolution in commercial Li-ion battery cells measured by on-line mass spectrometry – Effects of C-rate and cell voltage. *Journal of Power Sources* **477** (2020), 228968.

[6]   Berkes B.B., Jozwiuk A., Vračar M., Sommer H., Brezesinski T., Janek J.: Online continuous flow differential electrochemical mass spectrometry with a realistic battery setup for high-precision, long-term cycling tests. *Analytical Chemistry* **57** (2015), 5878–5883.

Modern techniques for the extraction and determination of the polyphenols in herbal matrices: a review

Kateryna Trach[a, *], Katarína Reiffová[a]

[a] *Department of Analytical Chemistry, Faculty of Science, Pavol Jozef Šafarik University in Košice, Moyzesova 11, 040 01 Košice, Slovak Republic ✉ kateryna.trach@student.upjs.sk*

Abstract
Numerous compounds comprising the polyphenol family are known to exhibit various health-promoting effects. Due to the latter, constant development of extraction, processing, and analysis techniques has been observed over the last two decades. Different types of such techniques have been developed to make polyphenolic compounds feasible for further use in the pharmaceutical, food, and chemical industries. The most widely used – solid phase microextraction (SPE), high-performance liquid chromatography with a diode array detector (HPLC-DAD) – as well as promising prospective techniques (for instance, magnetism-assisted solid phase microextraction or microwave hydrodiffusion and gravity extraction) have been studied and compared.

1. Introduction

Polyphenols are secondary metabolites of plants, with many pharmacological activities. Since many samples contain these compounds in trace or ultra-trace concentrations, and due to the complexity of herbal matrixes, the preparation of the pre-analysis sample is the most important step in the analysis of phenolic compounds in natural samples [1]. Liquid chromatography combined with electrospray ionization, triple quadrupole mass spectrometry, is a very sensitive tool used for polyphenols identification. High performance liquid chromatography combined with a photodiode-array (PDA) detector remains a technique that is used mainly for quantification of various phenolic compounds [2].

2. Current trends in sample preparation techniques

2.1 Advanced pretreatment methods

In general, any analytical method comprises two steps. The first step includes sample preparation of any kind and some extraction procedures. The latter was
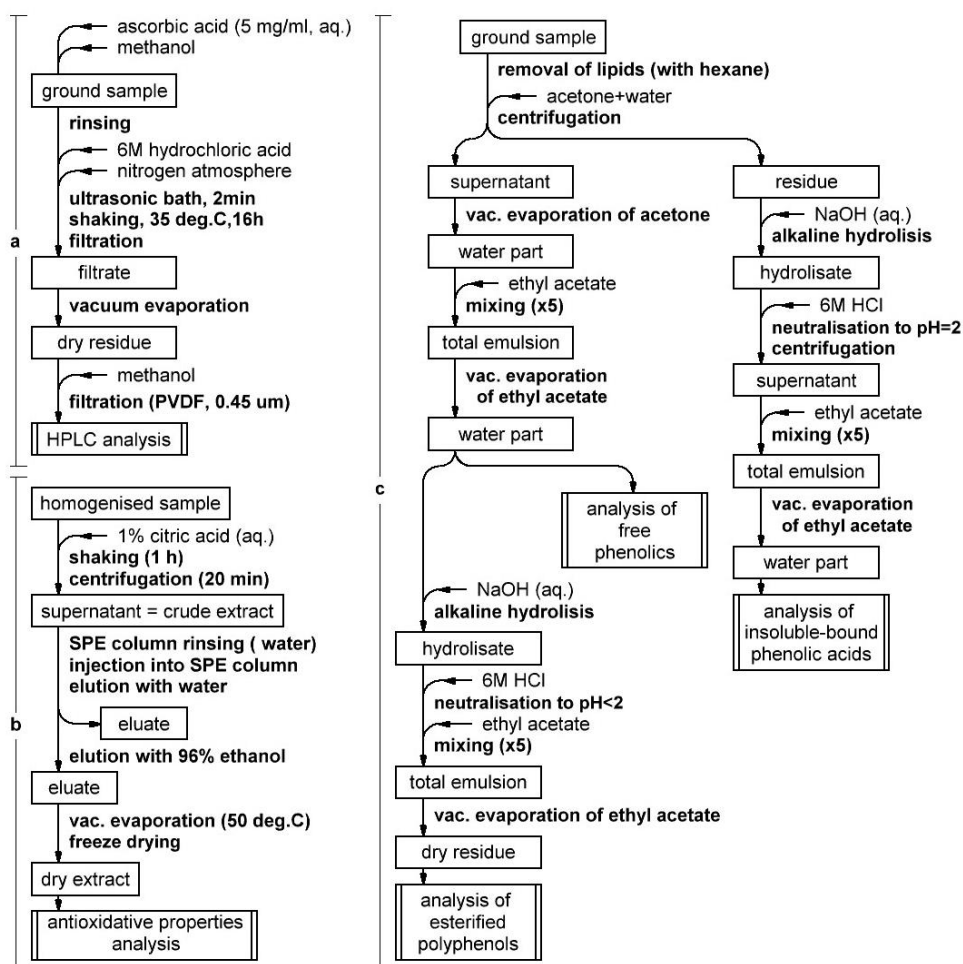
Fig. 1 Extraction and separation procedures of the polyphenols from berries: (a) classical extraction with ultrasonic-assisted extraction [3], (b) solid-phase extraction [4], and (c) classical extraction with sequential hydrolysis [5].

done to deal with problems associated with the matrix type, a small amount of analytes in real samples, or incompatibility of the analyte with the analytical method. The sample preparation plays a key role in the analysis process. It allows pre-concentration of the samples, increased precision and accuracy, and decreased interference. Figure 1 illustrates the basic steps of the most common polyphenol extraction methods in the example of berries.

Classical extraction techniques are ineffective, produce significant amounts of solvent waste, and thus are obsolete in terms of green analytical chemistry [6]. Therefore, it is important to find new ways for sample preparation techniques. The pulsed electric field (PEF) extraction is a selective technique that may be applied as a pretreatment process prior to conventional extraction. It was

reported to be an efficient method to increase phenolic content in fruit and vegetable samples. Among the advantages of this technique is the short extraction time, good effectiveness with a small amount of solvent, including cheap green solvents, and the possibility of the extraction process at ambient temperatures [7]. The authors [8] performed PEF pretreatment to determine the polyphenols of the beerd spent grain. As an extraction solvent, water was used. After pretreatment, extraction of the free fraction was performed using an ethanol/water solution. The phenolic compounds were determined by HPLC-mass spectrometry. Using this technique, the authors were able to improve total free phenolic recovery almost three times, compared to the samples without PEF treatment.

In electroporation process, the electric field impacts cell membranes, leading to pores formation in the cell membrane. Therefore, the permeability of the cell membrane is increased, which leads to a more efficient extraction of bioactive compounds from plant tissue. Electroporation was used for the extraction of polyphenols from *Vitis vinifera*, *Sideritis scardica* and *Crocus sativus* plants [9]. As the extraction solvent, water was chosen. Individual phenolic compounds were determined with HPLC-DAD.

The other two prospective technologies are ultrasound-assisted extraction (UAE) and microwave-assisted extraction (MAE). UAE is based on the effects of acoustic cavitation in the treated sample. This causes better interaction of the sample with the solvent and better extraction of compounds. MAE is based on heating of the extraction media using microwave energy. Ordoñez-Torres et al. [10] performed extraction of the polyphenols from mango peel by ultrasound microwave extraction, using methanol as a solvent. Polyphenolic compounds were identified afterwards by HPLC-electrospray ionization mass spectrometry (HPLC/ESI-MS) analysis. In [11] the extraction method for the determination of polyphenolic acids from different parts of *Nepeta cataria* L. was presented. Microextraction based on ultrasound-assisted vesicles with cetyl trimethyl-ammonium bromide vesicles and 5-methyl salicylic acid was performed. The detection of the compounds was performed by HPLC and dual absorbance detector. In the study [12], microwave-assisted extraction was used for the extraction of phenolic compounds from tomato. As a solvent, 80% methanol with 1% HCI was used. The phenolic compounds were determined by using Fourier-transform infrared spectroscopy and HPLC.

Another innovative extraction technique is microwave hydrodiffusion and gravity (MHG). The main advantage of this is that there is no need for solvent. The extraction occurs with "in situ" water. In the research [13], the content of poly-phenols in black mulberry (*Morus nigra* L. fruits) was analyzed. The extraction procedure was performed using a multimode microwave reactor. Individual polyphenols were analyzed using HPLC coupled with tandem MS (HPLC-MS/MS).

2.2. Usage of advanced solvents

Undoubtedly, solid-phase microextraction, or SPE, remains one of the most promising and reliable extraction techniques. In recent years, SPE methods have been reported with some features. For instantaneous, in [14] the authors have performed a preconcentration of quercetin using SHS-LLME (switchable hydrophilicity solvent-liquid-liquid microextraction), combined with DSPME (dispersive solid-phase microextraction). As SHS, the mixture of *N,N*-dimethylcyclohexylamine and 7.5 M nitric acid was utilized; 10.0 M sodium hydroxide was used as a phase separation trigger. The concentration of quercetin was determined with a UV / Vis spectrophotometer at 370 nm.

Another example of advanced technique is magnetism-assisted in-tube SPE performed by Chen et al. [15] for the determination of the phenolic acids in fruit juices. As a microextraction column, a capillary was used, packed with poly (1-allyl-3-methylimidazolium bis [(trifluoro methyl) sulfonyl] imide-co-ethylene dimethacrylate) monolith embedded with Fe_3O_4 nanoparticles, connected to a high-pressure pump. During extraction, variable magnetic fields were applied to the column by magnetic coil. Methanol was used for desorption. Polyphenolic acid quantification was performed by HPLC-DAD.

High molecular weight polymeric polyphenols, as well as low molecular weight ones linked to polysaccharides or proteins, also called nonextractable polyphenols (NEPs), are possible to extract with good yield using enzyme-assisted extraction. Domínguez-Rodríguez et al. [16] successfully determined NEPs in sweet cherry pomace with Depol and Promod enzymes. Deep eutectic solvents (DES) have also been used to extract phenolic compounds from rosemary and black mustard plants [17], food and beverages [18]. Choline chloride-based DES were used for this purpose [19].

3. Conclusions

Proper extraction is crucial for polyphenolic compounds, as their main sources are plant materials (plants, groceries, crops, etc.). Various methods such as CSE, LLME, MAE, UAE, and SPE have been successfully optimized to obtain the best yield and lowest compound degradation, while being cost-effective. Advanced methods such as UAE and MAE are considered to be faster, more efficient, and compatible with green chemistry principles. Moreover, such techniques lead to less degradation of extracted compounds. Further advancement is the use of modern solvents, for instance, SHS or DES. This approach has been proven to be intrinsically "green." It is worth to mention that several methods have been investigated as successful in the in-lab scale; however, they have limited possibilities to be up-scaled. Therefore, all techniques have their merits and drawbacks. The selection of a suitable technique should be made based on the plant matrix, the nature of the polyphenolic compound of interest, and the scale of the process.

References

[1]	Tashakkori P., Tagaç A.A., Merdivan M.: Fabrication of montmorillonite/ionic liquid composite coated solid-phase microextraction fibers for determination of phenolic compounds in fruit juices by gas chromatography and liquid chromatography. *Journal of Chromatography A* **1635** (2020), 461741.

[2]	Suleria H.A.R., Barrow C.J., Dunshea F.R.: Screening and characterization of phenolic compounds and their antioxidant capacity in different fruit peels. *Foods* **9** (2020), 1206.

[3]	Häkkinen S.H., Kärenlampi S.O., Heinonen M.I., Mykkänen H.M., Törrönen A.R.: HPLC method for screening of flavonoids and phenolic acids in berries. *Journal of the Science of Food and Agriculture* **77** (1998), 543–551.

[4]	Karabín M., Halama S., Jelínek L., Wang D., Dostálek P.: A comparison of Czech and Chinese varieties of barley with regards to technologically important polyphenolic substances. *Kvasný průmysl* **59** (2013) 346–351.

[5]	Denev P., Ciz M., Ambrozova G., Lojek A., Yanakieva I., Kratchanova M.: Solid-phase extraction of berries' anthocyanins and evaluation of their antioxidative properties. *Food Chemistry* **123** (2010), 1055–1061.

[6]	Sajid M., Płotka-Wasylka J.: Green analytical chemistry metrics: A review. *Talanta* **238** (2022), 123046

[7]	Ranjha M.M.A.N., Kanwal R., Shafique B., Arshad R.N., Irfan S., Kieliszek M., Kowalczewski P.Ł., Irfan M., Khalid M.Z., Roobab U., Aadil R.M.: A critical review on pulsed electric field: A novel technology for the extraction of phytoconstituents. *Molecules* **26** (2021), 4893.

[8]	Martín-García B., Tylewicz U., Verardo V., Pasini F., Gómez-Caravaca A.M., Cabonib M.F., Rosa M.D.:Pulsed electric field (PEF) as pre-treatment to improve the phenolic compounds recovery from brewers' spent grains. *Innovative Food Science & Emerging Technologies* **64** (2020), 102402.

[9]	Lakka A., Bozinou E., Makris D.P., Lalas S.I.: Evaluation of pulsed electric field polyphenol extraction from *Vitis vinifera, Sideritis scardica* and *Crocus sativus*. *ChemEngineering* **5** (2021), 25.

[10]	Ordoñez-Torres A., Torres-León C., Hernández-Almanza A., Flores-Guía T., Luque-Contreras D., Aguilar C.N., Ascacio-Valdés J.: Ultrasound-microwave-assisted extraction of polyphenolic compounds from Mexican "Ataulfo" mango peels: Antioxidant potential and identification by HPLC/ESI/MS. *Phytochemical Analysis* **32** (2021), 495–502.

[11]	Hajmohammadi M.R., AsliPashaki S.N., Dizavandi Z.R., Amiri A.: Ultrasound-assisted vesicle-based microextraction as a novel method for determination of phenolic acid compounds in *Nepeta cataria* L. samples. *Journal of the Iranian Chemical Society* **18**, 1559–1566.

[12]	Baltacıoğlu H., Baltacıoğlu C., Okur I., Tanrıvermiş A., Yalıç M.: Optimization of microwave-assisted extraction of phenolic compounds from tomato: Characterization by FTIR and HPLC and comparison with conventional solvent extraction. *Vibrational Spectroscopy* **113** (2021), 103204.

[13]	Mustafa A.M., Mazzara E., Abouelenein D., Angeloni S., Nunez S., Sagratini G., López V., Cespi M., Vittori S., Caprioli G., Maggi F.: Optimization of solvent-free microwave-assisted hydrodiffusion and gravity extraction of *Morus nigra* L. fruits maximizing polyphenols, sugar content, and biological activities using central composite design. *Pharmaceuticals* **15** (2022), 99.

[14]	Hassan M., Uzcan F., Shah S.N., Alshan U., Soylak M.: Switchable-hydrophilicity solvent liquid-liquid microextraction for sample cleanup prior to dispersive magnetic solid-phase microextraction for spectrophotometric determination of quercetin in food samples. *Sustainable Chemistry and Pharmacy* **22** (2021), 100480.

[15]	Chen H., Song X., Huang X.: Development of magnetism-assisted in-tube solid phase microextraction of phenolic acids in fruit juices prior to high-performance liquid chromatography quantification. *Journal of Separation Science* **44** (2021), 3418–3428.

[16] Dominguez-Rodriguez G., Marina M. L., Plaza M.: Enzyme-assisted extraction of bioactive non-extractable polyphenols from sweet cherry (*Prunus avium* L.) pomace. *Food Chemistry* **339** (2021), 128086.

[17] Serna-Vázquez J., Ahmad M.Z., Boczkaj G., Castro-Muñoz R.: Latest insights on novel deep eutectic solvents (DES) for sustainable extraction of phenolic compounds from natural sources. *Molecules* **26** (2021), 5037.

[18] Nia N.N., Hadjmohammadi M.R.: Development of magnetic dispersive micro-solid phase extraction based on magnetic adipic acid nanoparticles and deep eutectic solvents for the isolation and pre-concentration of phenolic compounds in fruit juice samples prior to determination by HPLC-UV. *Microchemical Journal* **170** (2021), 106721.

[19] Alam M. A., Muhhamad G., Khan M.N., Mofijur M., Lv Y., Xiong W., Xu J.: Choline chloride-based deep eutectic solvents as green extractants for the isolation of phenolic compounds from biomass. *Journal of Cleaner Production* **309** (2021), 127445.

Solvent impact and their elimination in liquid chromatography coupled with infrared spectroscopy for the identification of substances

Denis Pavelek[a], *, Radoslav Halko[a], Karatína Chovancová[a], Nicolas Milan Michalides[a]

[a] *Department of Analytical Chemistry, Faculty of Natural Sciences, Comenius University in Bratislava, Ilkovičova 6, 842 15 Bratislava, Slovak Republic ✉ pavelek7@uniba.sk*

Abstract
The analytical technique of combining liquid chromatography and infrared spectrometry is characterized by high chemical specificity, sensitivity, and qualitative as well as quantitative analysis of multicomponent mixtures. Separation of the individual components of the mixture is carried out through the separation capability of liquid chromatography, and their subsequent identification takes place using infrared spectrometry. The main problem in combining fluid chromatography with infrared spectrometry is a mobile phase (solvent) that can distort the infrared spectra analysed component of the mixture or analysed sample. Therefore, scientists are trying to eliminate the misrepresentation of infrared spectra samples solvents through a suitable interface. Whether it is direct measurements of the sample by flow cell, or offline, indirect measurement of the sample using solvent elimination method such as a hot gas stream or via ultrasonic sprayer.

1. Introduction

Fourier transform infrared spectroscopy (FTIR) is a nondestructive optical method that utilizes the infrared part of the electromagnetic spectrum in order to interact with molecules of substances. Radiation in the infrared region (IR) has a longer wavelength and lower frequency than radiation in the visible spectrum. When specific detection or identification of separated compounds is required, the combination of liquid chromatography (LC) and FTIR can prove beneficial [1]. With the high speed and wide range of applications of FTIR, spectra can be recorded at any time from a chromatogram. Due to several problems, including the absorption of IR radiation by the mobile phase, the combination of LC with FTIR is not at the same stage of development as the combination of gas
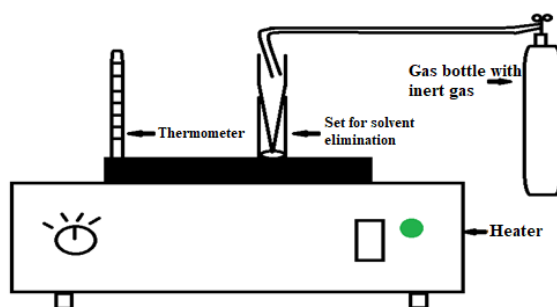
Fig. 1 Scheme of apparatus for solvent elimination method.

chromatography with FTIR [2, 3]. Because of this fundamental incompatibility, the combination of LC and FTIR has been the subject of research for more than twenty-five years. Almost all mobile phases used in LC absorb IR radiation at certain wavelengths, and because the mobile phase is present in a concentration much higher than that of the sample components, the sample spectra can only be obtained in spectral regions without solvent absorption bands (the IR spectra of the mobile phase overlap samples). For example, water and methanol, which are common polar solvents used in reverse phase-high-performance liquid chromatography (RP-HPLC), completely obscure solute bands throughout the spectrum. Therefore, observation and identification of trace compounds in the presence of the LC mobile phase is a major problem when using IR detection in the LC [3–5]. The solution to this problem can be implemented in two ways:

1. Flow cells are used to collect the eluent from the LC column and continuously record the IR spectrum using FTIR. On the contrary, the disadvantage of using flow cells in LC-FTIR is the high limit of detection (LOD) of analytes; on the other hand, they can be useful for quantitative and specific identification of the primary components of a mixture [2, 6].

2. The second method works on the principle of eliminating the LC solvent before infrared detection using an interface that evaporates the eluent and deposits analytes on the substrate (Fig. 1). Solvent elimination techniques provide much better detection sensitivity and increase spectral quality, which is essential when unambiguous identification of sample components at low concentration levels is required [7].

An additional method for preparing samples for LC and FTIR is single drop extraction or liquid-liquid microextraction using a nonpolar agent.

2. Experimental

2.1 Materials

Deionized water prepared by Water for PS, ethanol, caffeine, citric acid, L(+)-ascorbic acid, L(+)-tartaric acid, vitamin B17 amygdalin, vitamin D_3,

methanol 99% for gradient elution, acetonitrile 99% for gradient elution, lactic acid, formic acid 85%, acetic acid 100%, phosphoric acid 85%, ammonium formate, ammonium acetate, ammonium dihydrogenphosphate, glucose, tetra-methylamonium iodide, salicylic acid, vitamin B_{12}, malic acid, bis(cyclohexa-none)oxaldihydrazone, perfluoropropyl iodide, perfluorohexyl iodide, 1-bromo-heptadecafluorooctane.

2.2 Preparation of solutions

Determination of the LOD of various analytes with IR spectrometry with transflective (R-A) technique: we prepared stock aqueous solutions from caffeine, citric acid, L(+)-ascorbic acid, L(+)-tartaric acid and amygdalin to 100 mL of a volumetric flask with a concentration of 1 mmol L^{-1}. Subsequently, we diluted them to a concentration of 0.1 and 0.5 mmol L^{-1}.

Study of the influence of solutions on the infrared spectrum of analytes with IR spectrometry with the R-A technique: Mobile phases were prepared as mixtures: water:methanol, water:ethanol, water:lactic acid and water:acetonitrile in ratio 40:60 (*v/v*). At the same time, a stock solution of L(+)-ascorbic acid was prepared with concentration of 10 mmol L^{-1}. The fractions of L (+)-ascorbic acid were diluted in mobile phases with concentration of 1 mmol L^{-1} and 0.1 mmol L^{-1}.

Study of the influence of buffers on the infrared spectrum of analytes with IR spectrometry with the R-A technique: Three different buffers were prepared, which were composed of weak acid and its salt: formic acid and ammonium formate, acetic acid and ammonium acetate and phosphoric acid and ammonium dihydro-genphosphate with concentration of 10 mmol L^{-1}. The pH of buffer solutions was adjusted by using their appropriate acid. The mobile phases consisted of methanol and prepared buffers in ratio 60:40 (*v/v*). A stock solution of L(+)-ascorbic acid was prepared with concentration of 10 mmol L^{-1}. The fractions of L (+)-ascorbic acid were diluted to mobile phases with concentration of 1 mmol L^{-1}.

Liquid-liquid microextraction: Various standard solutions were prepared using caffeine, glucose, iodide tetramethyl, salicylic acid, vitamin B_{12}, malic acid, bis(cyclohexanone)oxaladihydrazone, amygdalin and ascorbic acid dissolved in water that were made at different concentrations (1, 5, 10, 15, 20, 25, 30 g μL^{-1}). Next, we prepared three groups of solutions comprising each of the analytes dissolved in water with a concentration of 20 g μL^{-1} and non-polar extraction reagents:perfluoropropyl iodide, perfluorohexyl iodide, 1-bromohepta-decafluorooctane.

3. Results and discussion

3.1 Determination of the LOD of various analytes with IR spectrometry with transflective (R-A) technique

Using FTIR with the R-A technique, we determined the *LOD* of various analytes, that is, we determined the smallest amount of sample that could possibly be detected. The aqueous solutions were gradually dosed into a pre-produced set for solvent elimination with a nitrogen stream and a temperature on aluminium foil as a substrate R-A with volume of 0.5; 1; 5; 10; 20 and 30 μL. During solvent evaporation, the heater was set at 100° C, but the actual thermometer reading was 82° C. A reflection mode R-A technique has been used to record the IR spectrum of the analyte after drying the sample. As a result of all measurements, we determined the smallest quantities of each sample that can be detected, based on the quality of the IR spectrum.

Our objective in this section was to investigate the impact of various compositions of mobile phases, which are commonly used in LC, on the IR spectrum of analytes. As a combination of RP-HPLC and infrared spectrometry, appropriate polar solvents with low boiling points should be selected. As polar solvents overlap their characteristic absorption strips in the IR spectrum, the analyte must be completely eliminated from the solvent. Several mobile phases were utilized for the separation of the analytes due to their low boiling points and purity, namely, water:methanol and water:acetonitrile. The pollution of the mobile phase water:ethanol was high, which was also reflected in the quality of the IR spectrum of the measured analyte. A similar problem was also encountered in mobile phase water:lactic acid, where the high boiling point of the lactic acid led to deterioration of the IR spectrum of the analyte due to improper evaporation of the lactic acid.

3.2 Study of the influence of buffers on infrared spectrum of analytes with IR spectrometry with the R-A technique

The purpose of this section was to study the impact of buffers on the IR spectrum of analytes. Buffers present a problem in combination with LC and IR spectrometry, since they tend to form salt crystals during solvent removal as they are derived from buffering solutions, where a weak acid or base is evaporated due to their low boiling points. Salt crystals can leave their characteristic absorption strips in the IR spectrum of the analyte and cover the characteristic absorption strips of the measured analyte, since they absorb IR radiation as well. Ammonium acetate and ammonium formate left some characteristic absorption strips in the IR spectrum of the analyte, but the IR spectrum of ammonium dihydrogen-phosphate has covered the whole IR spectrum of the analyte.

The qualitative analysis was performed using all previously conducted studies with an offline combination of LC and IR spectrometry applied to selected commercial nutritional samples. When selected fractions of amygdalin, cholecalciferol, and cytosan nutritional samples, we were able to eliminate their solvents and determine their IR spectra. By combining four analytes, caffeine, L(+)-ascorbic acid, L(+)-tartaric acid, and amygdalin, we were also able to obtain individual fractions, which were analyzed by infrared spectroscopy.

3.3 Liquid-liquid microextraction

The following nine series of standard solutions were prepared with caffeine, glucose, tetramethylamonium iodide, salicylic acid, vitamin B_{12}, malic acid, bis(cyclohexanone)-oxaladihydrazone, amygdalin, and ascorbic acid dissolved in water. The solutions were prepared at different concentrations (1, 5, 10, 15, 20, 25 and 30 $g\,\mu L^{-1}$). Ultraviolet spectrometric analysis of standard solutions was performed, and after analysis, a calibration curve was produced based upon the dependence of absorbance to concentration of analytes in standard solutions. Subsequently, we performed L-L microextraction using nonpolar reagents (perfluoropropyl iodide, perfluorohexyl iodide, 1-bromoheptadecafluorooctane) dissolved in water with a concentration of 20 $g\,\mu l^{-1}$. The organic phase was removed after extraction, and by using ultraviolet spectrometry, the absorbance was measured, and the recovery was calculated for each aqueous phase. As a nonpolar extraction reagent, 1-bromoheptadecafluorooctane had the highest recovery when used in a series of solutions.

4. Conclusions

Through the use of studies and experiments performed, it was possible to optimize the RP-HPLC-FTIR method using solvent elimination by gas stream and liquid-liquid microextraction for the analysis of multicomponent samples.

References

[1]　Somsen G.W., Gooijer C., Brinkman U.A.: Liquid chromatography–Fourier-transform infrared spectrometry. *Journal of Chromatography A* **856** (1999), 213–242.
[2]　Fujimoto G., Uematsu G., Jinno K.: The use of deuterated solvents in high-performance liquid chromatography-Fourier transform infrared spectrometry. *Chromatographia* **20** (1985), 112–116.
[3]　Fujimoto C., Oosuka T., Jinno K.: A new sampling technique for reversed-phase liquid chromatography/fourier-transform infrared spectrometry. *Analytica Chimica Acta* **178** (1985), 159–167.
[4]　Jones J.C., Littlejohn D., Griffiths P.R.: Comparison of solvent elimination systems for the analysis of dyes and pesticides by high-performance liquid chromatography Fourier transform infrared spectrometry. *Applied Spectroscopy* **53** (1999), 792–799.

[5]   Taylor S.D.: In-line combination of LC with MS, NMR, UV and IR in drug analysis. *Doctoral thesis*. Sheffield Hallam University 2007. http://shura.shu.ac.uk/id/eprint/20429

[6]   Jinno K., Fujimoto C.: Coupling of microcolumn high-performance liquid chromatography with Fourier transform infrared spectrometry. *Journal of Chromatography A* **506** (1990), 443–460.

[7]   Tran C.D., Huang G., Grishko V.I.: Direct and indirect detection of liquid chromatography by infrared thermal lens spectrometry. *Analytica Chimica Acta* **299** (1995), 361–369.

Determination of cadmium by chemical vapour generation coupled with atomic fluorescence spectrometry

Barbora Štádlerová[a, b, *], Linda Sagapova[a, b], Stanislav Musil[a]

[a] *Institute of Analytical Chemistry of the Czech Academy of Sciences, Veveří 97, 602 00 Brno, Czech Republic* ✉ *stadlerova@iach.cz*
[b] *Department of Analytical Chemistry, Faculty of Science, Charles University, Hlavova 8/2030, 128 43 Prague 2, Czech Republic*

Keywords

atomic fluorescence
    spectrometry
cadmium
chemical vapour
    generation

Abstract

Chemical vapour generation of cadmium in a four-channel system using Cr^{3+}/KCN as additives was successfully coupled to an in-house constructed nondispersive atomic fluorescence spectrometer. The atomization conditions in two atomizers – a miniature diffusion flame and a flame-in-gas-shield atomizer – were optimized. Interfering effects of several hydride forming elements were studied and it was found that Sn, Sb, As, Bi, Hg and Se exhibited no interference on Cd determination up to $100~\mu g\,L^{-1}$ while significant interference (response decreased by 13%) was identified for Pb even at $10~\mu g\,L^{-1}$. The limits of detection were 1.4 and $0.42~ng\,L^{-1}$ for the miniature diffusion flame and the flame-in-gas-shield atomizer, respectively. The accuracy of the developed methodology employing the flame-in-gas-shield atomizer was successfully verified by analysis of a certified reference material of fresh water NIST 1643f.

1. Introduction

Cadmium is a toxic and carcinogenic metal that is considered one of the most common environmental pollutants. It is easily transported from water and soils to plants and ultimately humans through food intake, e.g., rice. The ingestion of Cd may cause lung cancer, renal dysfunction or hypertension [1, 2]. The Cd tolerable monthly intake was set to be $25~\mu g\,kg^{-1}$ body weight and the EU limits of Cd content in food are, e.g., $0.05~\mu g\,kg^{-1}$ in meat and $0.2~\mu g\,kg^{-1}$ in rice [3]. The concentration in food varies a lot and it is therefore important to develop methods with sufficiently low limits of detection.

Chemical vapour generation employing the reaction of acidified analyte with sodium borohydride coupled to analytical atomic spectrometry is advantageous because the analyte is efficiently converted to volatiles species, separated from the liquid matrix and very efficiently transported into the detector. Cadmium is not a

typical hydride forming element such as As, Se, and Bi, and the chemical vapour generation efficiency remains unsatisfactory when chemical vapour generation is conducted by means of only acid and sodium borohydride. The use of additives, such as Co^{2+} ions, Ti^{4+}/KCN or Cr^{3+}/KCN can significantly enhance the generation efficiency and thus improve the overall performance [4]. Furthermore, the coupling of this approach to detectors such as atomic fluorescence spectrometry allows reaching extremely low limits of detection and therefore performance-wise it can compete with inductively coupled plasma mass spectrometry (ICP-MS), the usual tool for ultra-trace element analysis, but at much lower investment and running costs [5].

The aim of this work was to develop a methodology for Cd determination at ultra-trace levels based on chemical vapour generation in the presence of additives coupled with atomic fluorescence spectrometry. Two atomizers were employed, the miniature diffusion flame (MDF) and the flame-in-gas-shield (FIGS) atomizer, and the conditions of atomization were optimized. The analytical charac-teristics were determined and the methodology was applied to water analysis.

2. Experimental

2.1 Reagents and chemicals

Ultrapure water Analpure (Analytika, Czech Republic) was used for the preparation of all solutions. A 5% (m/v) $NaBH_4$ (≥99%, Honeywell, USA) in 0.4% (m/v) KOH (semiconductor grade, Sigma-Aldrich, Germany) was used as a reducing agent. A solution of 0.2 mol L^{-1} HCl (Merck, Germany) was used as a carrier/blank. Working 250 ng L^{-1} Cd solution was prepared fresh daily by serial dilution of a 1000 mg L^{-1} Cd standard (Analytika, Czech Republic). The additives were prepared as follows: 0.6 mmol L^{-1} working Cr^{3+} solution and 24 mmol L^{-1} modifying solution from solid $Cr(NO_3)_2 \cdot 9H_2O$ (Sigma-Aldrich, Germany), and 10 mmol L^{-1} working KCN solution from solid KCN (Acros Organics, USA).

2.2 Atomic fluorescence spectrometer

A nondispersive atomic fluorescence spectrometer constructed at our laboratory, described in detail in our previous work [6], was employed. A Cd electrodeless discharge lamp (Perkin-Elmer, System 2) was used and the operating current was 240 mA. The photomultiplier tube was placed perpendicularly to the lamp to collect the fluorescence radiation emitted from the atomizer. The fluorescence radiation passed through an interference filter (228 nm, FWHM 10 nm, Melles Griot), covering the Cd fluorescence line at 228.8 nm, and was then focused into a solar-blind photomultiplier tube (MH 1922, 165–320 nm, Perkin-Elmer Opto-electronics, USA).
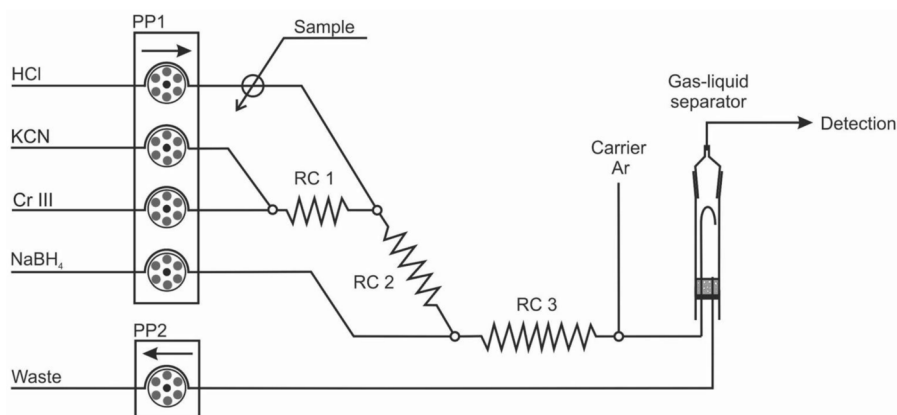
Fig. 1 Four channel chemical vapour generator: (PP) peristaltic pump, (RC) reaction coil.
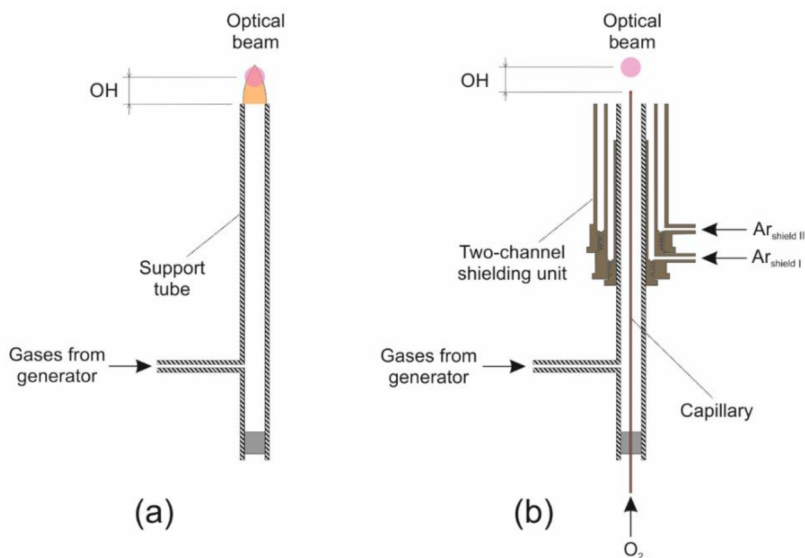
Fig. 2 Atomizers used in this work: (a) the miniature diffusion flame, and (b) the flame-in-gas-shield atomizer; (OH) observation height.

2.3 Hydride generator and atomizers

A four-channel flow injection chemical vapour generator was employed (Fig. 1). The reducing agent and the carrier (both 1 mL min^{-1}) and the additives KCN and Cr^{3+} (both 0.5 mL min^{-1}) were pumped by a peristaltic pump Reglo Digital (Ismatec, Switzerland). The manifold was constructed from PTFE tubing (1 mm i.d.). The sample was injected through a 0.15 mL sample loop into the flow of a carrier and subsequently merged with the other reagents. A glass gas-liquid

separator (5 mL) with a forced waste removal was employed in order to separate the gas phase containing volatile cadmium species employing carrier argon (80 mL min^{-1}). The amount of hydrogen evolving from the reaction was 20 mL min^{-1}. The gas phase exiting the gas-liquid separator was supplied with an additional flow of argon and hydrogen to maintain a stable flame of the atomizer. Two atomizers were employed: MDF and FIGS atomizer (Fig. 2). MDF consisted of a vertical quartz support tube (6 mm i.d.) with a side inlet arm through which argon, hydrogen and the analyte were introduced. The observation height was defined as the distance from the top of the support tube to the centre of the optical beam. Regarding FIGS, there was an additional capillary (i.d. 0.53 mm) in the axis of the support tube protruding 3 mm above the rim of the support tube, serving to introduce oxygen at low flow rate. A two-channel brass shielding unit was fitted around the support tube through which shielding flows of argon were introduced [7].

2.4 Procedure and data evaluation

The standard was injected 10 s after the signal recording had started (90 s recording). The detector output provided signals in μV. Peak area (μV s) corrected to baseline, or sensitivity (μV s L ng^{-1}), and a signal to noise ratio were the parameters used to evaluate the data. Signal to noise ratio was determined by dividing the peak area by an average standard deviation of blank (three replicates of 10 s).

Prior to any experiment, it was necessary to modify the chemical vapour generation system with 24 mmol L^{-1} Cr^{3+} solution in order to reach desired sensitivity [4]. After modification the concentration of Cr^{3+} was decreased to 0.6 mmol L^{-1} and employed throughout all the measurements.

3. Results and discussion

A four-channel generator was coupled to the in-house constructed non-dispersive atomic fluorescence spectrometer. The Cr^{3+}/KCN modifier was selected to support chemical vapour generation as it was shown to enhance the overall chemical vapour generation efficiency to almost 70% [4]. Both the excitation and fluorescence radiation were focused correspondingly and the feeding current of the electrodeless discharge lamp was optimized in order to yield maximum sensitivity. Cd detection by atomic fluorescence spectrometry is extremely sensitive, which is obviously an advantage; on the other hand, the contamination issues need to be treated. It is crucial to use reagents of the highest purity to suppress the contribution of Cd contamination to measured background and thus reach as high signal to noise ratio and low limit of detection as possible.

The atomization conditions were optimized using a 250 ng L^{-1} Cd standard solution: total flow rate of argon and hydrogen, hydrogen fraction and the observation height for both flame atomizers. Additionally, the oxygen flow rate

Table 1

Optimum atomization conditions.

Parameter	Atomizer	
	Miniature diffusion flame	Flame-in-gas-shield
Ar / mL min^{-1}	435	345
H$_2$ / mL min^{-1}	65	55
O$_2$ / mL min^{-1}	n/a	12
Ar$_{shield\ I}$; Ar$_{shield\ II}$ / mL min^{-1}	n/a	1.5; 1.5[a]
Observation height / mm	7	7

[a] Optimum Ar$_{shield}$ flow rates taken from [7].

was optimized for FIGS. Firstly, the hydrogen fraction was optimized in the range from 17% to 50% for MDF and from 11% to 25% for FIGS at constant total gas flow rate. The sensitivity and signal to noise ratio generally increase with lower hydrogen fraction, hence 17% and 13% were selected as optimum for MDF and FIGS, respectively, as these values were the lowest possible at which the flame remained stable. Total gas flow rate and observation height was then optimized at constant hydrogen fraction. It was found that the optimum is 400 mL min^{-1} for both atomizers at the observation height of 7 mm. The oxygen flow rate through the capillary of the flame-in-gas-shield atomizer was optimized separately and 12 mL min^{-1} were selected as optimum. Optimum conditions are summarized in Table 1.

Interference from several hydride forming elements (Pb, Sn, As, Se, Sb, Bi) and Hg was investigated at three concentration levels (1, 10 and 100 µg L^{-1}). There was no interference observed from all the elements with the exception of Pb for which the response of Cd was suppressed by circa 13% at 10 µg L^{-1} in the case of both flame atomizers.

Analytical characteristics were determined for both atomizers. The limit of detection achieved with the FIGS (0.42 ng L^{-1}) was circa 3 times lower than with MDF (1.40 ng L^{-1}). These limits of detection compete well with the typical limits of detection of much more costly methods such as ICP-MS. In addition, the instrumental limit of detection (blanks measured when the generator was switched off) was assessed as 0.1 ng L^{-1}. We can deduce that the limits of detection are mostly limited by Cd contamination present even in the trace element analysis grade reagents.

Last but not least, Cd content was determined in the standard reference material NIST 1643f (fresh water). The concentration measured by chemical vapour generation-atomic fluorescence spectrometry corresponded to (5.90±0.44) µg L^{-1} which is in very good agreement with the certified value (5.89±0.13) µg L^{-1}. The recovery from the 30-fold diluted sample medium, calculated from the ratio of slope of the standard additions (two spiked concentrations) and external calibration functions, was 108±2%.

4. Conclusion

An ultrasensitive methodology for cadmium determination by chemical vapour generation coupled with atomic fluorescence spectrometry was successfully developed. The atomization parameters of two atomizers – the miniature diffusion flame and the flame-in-gas-shield atomizer – were optimized. An interference study was carried out and there were no interferences observed from Hg, Sb, Se, Bi, Sn and As but a negative interference from Pb was observed. The flame-in-gas-shield atomizer was further employed to verify the accuracy by analysis of water certified reference material as it delivered desired sensitivity and lower limit of detection (below 1 ng L^{-1}). The next step is to apply this method to Cd determination in real samples, preferably rice.

References

[1] Uraguchi S., Fujiwara T.: Cadmium transport and tolerance in rice: perspectives for reducing grain cadmium accumulation. *Rice* **5** (2012), 5.

[2] Kato L.S., Fernandes E., Raab A., Bacchi M., Feldmann J.: Arsenic and cadmium contents in Brazilian rice from different origins can vary more than two orders of magnitude. *Food Chemistry* **286** (2019), 644-650.

[3] *Commission Regulation (EC) No 1881/2006 of 19 December 2006 setting maximum levels for certain contaminants in foodstuffs.* https://eur-lex.europa.eu/legal-content/EN/ALL/-?uri=celex%3A32006R1881. Accessed on 20 June 2022.

[4] Sagapova L., Musil S., Kodríková B., Svoboda M., Kratzer J.: Effect of additives on cadmium chemical vapor generation and reliable quantification of generation efficiency. *Analytica Chimica Acta* **1168** (2021), 338601.

[5] Dědina J.: Atomization of volatile compounds for atomic absorption and atomic fluorescence spectrometry: on the way towards the ideal atomizer. *Spectrochimica Acta B* **62** (2007), 846–872.

[6] Musil S., Matoušek T., Currier J.M., Stýblo M., Dědina J.: Speciation analysis of arsenic by selective hydride generation-cryotrapping-atomic fluorescence spectrometry with flame-in-gas-shield atomizer: achieving extremely low detection limits with inexpensive instrumentation. *Analytical Chemistry* **86** (2014), 10422–10428.

[7] Štádlerová B., Kolrosová M., Dědina J., Musil S.: Atomic fluorescence spectrometry for ultrasensitive determination of bismuth based on hydride generation – the role of excitation source, interference filter and flame atomizers. *Journal of Analytical Atomic Spectrometry* **35** (2020), 993–1002.

Trapping of volatile cadmium species on gold surfaces for atomic absorption spectrometry

Linda Sagapova[a, b, *], Milan Svoboda[a], Tomáš Matoušek[a], Jan Kratzer[a]

[a] *Institute of Analytical Chemistry of the Czech Academy of Sciences, Veveří 97, 602 00 Brno, Czech Republic ✉ sagapova@iach.cz*
[b] *Department of Analytical Chemistry, Faculty of Science, Charles University, Hlavova 8/2030, 128 43 Prague 2, Czech Republic*

Keywords
atomic absorption
    spectrometry
cadmium
chemical vapor
    generation
preconcentration

Abstract
Simple preconcentration step was developed for cadmium determination after chemical vapor generation prior to atomic absorption spectrometric detection. Chemical vapor generation of cadmium was performed in the presence of Cr^{3+}/KCN as modifiers. The vapor generation system was connected to the quartz modular trap-and-atomizer device allowing for direct analyte preconcentration in the independently heated inlet arm of this device. Gold amalgamators or nanoparticles were tested as preconcentration surfaces. Efficient cadmium trapping was observed on gold amalgamators followed by unsuccessful analyte release. Key-parameters were optimized for gold nanoparticles including the temperature of trapping (200 °C) and volatilization (900 °C) steps, the carrier gas composition and its flow rate as well as the amount of gold nanoparticles (8 μg Au). Limit of detection reached in this arrangement was 13 pg mL^{-1} Cd, being approximately 5-times better than in the mode without any preconcentration. The efficiency of cadmium preconcentration step with gold nanoparticles was estimated to 70%.

1. Introduction

Cadmium and its compounds have been classified as carcinogenic by the International Agency for Research on Cancer, primary associated with human lung, prostate, and recently pancreatic cancer [1]. As a consequence, development of sensitive and fast methodology for cadmium determination is still desirable. Chemical vapor generation coupled with atomic absorption spectrometry (AAS) was in detail optimized in our laboratory recently [2]. In the presence of Cr^{3+}/KCN as modifiers the efficiency of the generation step was as high as 60%. Providing chemical vapor generation is combined with an efficient preconcentration step, an analytical method suitable for routine cadmium determination can be developed even with the simple and cheap AAS detector. Such a combination can compete in analytical performance with much more expensive and sophisticated

ICP-MS detector with liquid sample nebulization. Gold appears to be a suitable preconcentration surface for a number of metals after chemical vapor generation step. Due to its ability to form amalgams, gold was reported to efficiently preconcentrate cold vapors of Hg [3] and hydrides of As [4], and Se [5].

The aim of this work was the evaluation of gold-based materials targeting the most efficient and sensitive approach to cadmium preconcentration compatible with chemical vapor generation and AAS detection. Analytical figures of merit were subsequently evaluated and compared to those for chemical vapor generation-AAS without any preconcentration.

2. Experimental

2.1 Reagents and chemicals

Boiled and deaerated (30 min by a 100 mL min^{-1} stream of Ar) deionized water (< 0.1 μS cm^{-1}, Ultrapur, Watrex, USA) was used to prepare all solutions. Working cadmium standards were prepared by a dilution from 1000 μg mL^{-1} Cd stock solution (Astasol, Analytika, Czech Republic) in 0.2 mol L^{-1} HCl. Hydrochloric acid (37%, p.a.) was sourced from Merck (Germany). Solid NaBH$_4$ ($\geq$ 97%, Sigma-Aldrich, Germany) was used to prepare a fresh solution of 5% (m/v) NaBH$_4$ in deionized water stabilized by 0.4% (m/v) KOH (p.a., Merck, Germany). Solutions of modifier Cr^{3+} (0.04 mol L^{-1} and 0.001 mol L^{-1} Cr^{3+}) were prepared from Cr(NO$_3$)$_3$·9H$_2$O ($\geq$ 99.99% trace metal basis, Sigma-Aldrich, Germany). Solution of 0.1 mol L^{-1} KCN ($\geq$ 97.0%, Fluka, Switzerland) was used as a second modifier. A mixture 3:7 (v/v) of HF (38%, Spolchemie, Czech Republic) and HNO$_3$ (65%, Lach-Ner, Czech Republic) was used to everyday clean the quartz modular trap-and-atomizer device prior to its use. Gold nanoparticles solution (60 nm, stabilized suspension in citrate buffer, Sigma-Aldrich, Germany), and a gold amalgamator filling (gold coated alumina, mean Al$_2$O$_3$ size 150 μm, 10% Au) from Altec, Czech Republic, were used for preconcentration.

2.2 Instrumentation

2.2.1 Atomic absorption spectrometry

The Perkin-Elmer model 503 atomic absorption spectrometer (Bodenseewerk, Germany) was employed without background correction and equipped with a Cd electrodeless discharge lamp (Perkin-Elmer, USA) operated at 240mA. All measurements were performed at 228.8 nm using a 0.7 nm as the spectral bandwidth.

2.2.2 Generator

Four channel chemical vapor generation system was in detail described in our recent paper [2].

2.2.3 Trap-and-atomizer device

The modular trap-and-atomizer device is derived from the design of a multiple microflame atomizer [6, 7], which is an advanced construction of an externally heated quartz tube atomizer. Compared to the common multiple microflame atomizer the only difference is that its inlet arm is not firmly sealed to the optical arm, but is simply demountable and connectable. Consequently, its inner surface can be easily modified or filled by various materials to improve the preconcentration efficiency. The inlet arm (trap) is a bare quartz tube of 65 mm length (2 mm i.d., 4 mm o.d.) which can be heated resistively to any desired temperature between ambient and 900 °C independently of the optical arm.

The trap is heated by a Ni-Cr wire (2.7Ω m^{-1}; 0.65 mm diameter, ElchemCo, Czech Republic) using a laboratory power source (HCS-3202, Manson Engineering Industrial, China) controlled by a home-made one button relay device. Every new trap is calibrated with with a digital thermometer (Cole Parmer, Digi-Sense 8528-20, USA) equipped with a K-type thermocouple (Omega Engineering, USA).

Two preconcentration surfaces were tested in this work.

Gold amalgamators are commercially available (Altec, Czech Republic) to be used in a single purpose mercury analyzer AMA-254. The quartz tube of the same dimensions as described above is purchased already packed with circa 100 mg of the gold-coated alumina filling.

The traps treated with gold nanoparticles commercial solution were prepared as follows: a maximum volume of 50 µL of gold nanoparticles solution was injected into the trap (emptied and pre-cleaned amalgamator tube made of quartz) by a Hamilton syringe and left to dry in an oven at 80 °C for 4 hours. The whole procedure was repeated if necessary to reach the desired gold nanoparticles volume (up to 300 µL, i.e., 6 times).

The optical arm served as an atomizer. It was heated to 900 °C by an electrically heated cell assembly (Perkin Elmer) controlled by the MSVT-1 controller (UIACH of the CAS, Czech Republic).

2.3 Procedure

The preconcentration procedure consisted of two steps, analyte trapping and subsequent volatilization, regardless of the nature of preconcentration material tested.

Trapping step: after the previous replicate measurement the trap is cooled down for 120 s from the volatilization temperature (900 °C) to reach the trapping temperature (200 °C). The peristaltic pump is switched on to introduce Cd standard solution or blank (60 s).

Volatilization step: the inlet arm is heated resistively to the volatilization temperature (900 °C) for 11 s. The signal acquisition started, at the same time with

the trap heating. The signal integration period was 100 s. After each measurement the Cd sample was replaced by the blank for 60 s to flush all the analyte from the generator.

If explicitly stated, measurements were performed in the mode without preconcentration in order to compare sensitivity (or peak area) reached for the same analyte amount and to deduce the preconcentration efficiency. In such a case, the inlet arm was not modified (empty quartz trap) and the trap heating was off.

3. Results and discussion

3.1 Gold amalgamator

Gold coated alumina (amalgamator filling) was studied due to the chemical similarity of cadmium and mercury. Studied parameters for trapping and volatilization were: heating rate and temperature value, gas phase composition and trapping capacity. Subsequently, the trapping and volatilization efficiency was quantified by leaching the amalgamator filling (10% HNO_3) followed by quantification of cadmium fraction in the leachate by ICP-MS/MS. The possibility of AAS measurements was limited since it was not possible to detect cadmium signal in the volatilization step. This led to the hypothesis the interaction between trapped cadmium species and gold amalgamator is so strong that their release cannot be achieved. AAS detector was used to monitor the non-retained cadmium fraction in the trapping step. However, no "breakthrough" signal was observed indicating efficient cadmium trapping. As a consequence, leaching experiments with ICP-MS detection were performed to gain more insights into the preconcentration in the gold amalgamators instead of AAS measurements.

Two sets of experiments have been performed in which the amalgamator filling was leached either after the trapping step, or after the whole preconcentration procedure, i.e., trapping and subsequent volatilization step. It was found that the amalgamator filling is capable of efficient capture of cadmium in a wide temperature range (25–900 °C) and has sufficient capacity to preconcentrate trace amounts of cadmium (more than 15 ng Cd). Trapping efficiency was quantified to (98±21)%. However it was not possible to subsequently release the analyte from the amalgamator trap under any conditions. Maximum volatilization temperature of 900°C was applied using 100% H_2 atmosphere. Despite these volatilization conditions, the fraction of cadmium found in the leachate was quantified to (103±14)% of the generated analyte indicating any release of cadmium. As a consequence, amalgamator filling was not tested further as a preconcentration surface.
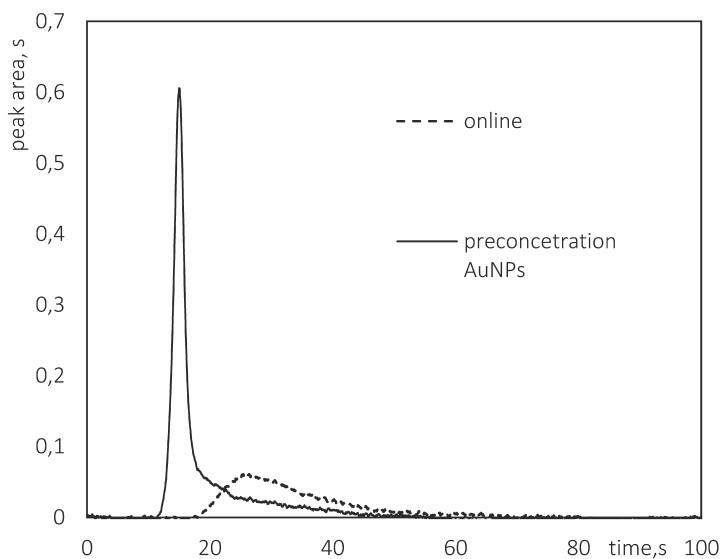
Fig. 1 Comparison of peak signals acquired by chemical vapor generation-atomic absorption spectrometry in the on-line (no preconcentration) mode and preconcentration mode (gold nanoparticles) for $0.3\ \mu g\,L^{-1}$ cadmium standard (0.45 ng Cd).
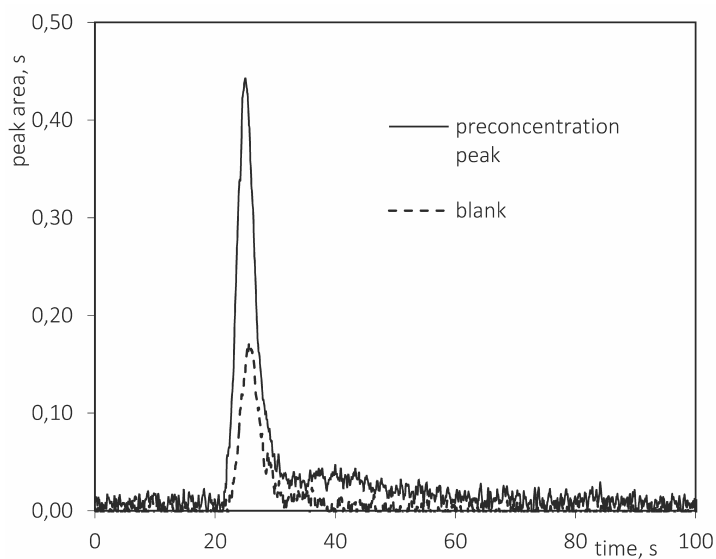

Fig. 2 Signal of $0.1\ \mu g\,L^{-1}$ Cd standard solution (0.15 ng Cd) and a blank in the after preconcentration on gold nanoparticles.

3.2 Gold nanoparticles

The measurements were performed with AAS detection according to the procedure described in section 2.3. The experimental conditions were optimized as follows: trapping temperature 200 °C, volatilization temperature 900 °C, the composition and flow rate of carrier gas 75 mL min^{-1} Ar and 20 mL min^{-1} H$_2$. The volume of gold nanoparticles solution employed for inner surface modification of the quartz trap was optimized to 300 μL, corresponding thus to 8 μg Au.

The preconcentration efficiency under the optimum conditions was estimated to 70%. Limit of detection reached 13 pg mL^{-1} Cd. Figure 1 compares the peak shapes in the modes with and without preconcentration prior to AAS detection.

Within all measurements based on gold nanoparticles, it was necessary to correct the results to a blank value which was relatively high even under the optimized conditions (Fig. 2). The explanation is not known yet. Most likely is the increased blank value related to the contamination of the chemicals (modifiers) by cadmium and the fact an on-line synthesized K$_3$Cr(CN)$_6$ is partially hydrolyzed in the gas-liquid separator to Cr(III) hydroxide being continuously formed and dissolved in the chemical vapor generation system.

4. Conclusion

A fast and simple cadmium preconcentration step, performed after chemical vapor generation in the gas phase, was developed employing a modular trap-and-atomizer device. Gold nanoparticles were found as the best preconcentration surface. The limit of detection of 13 pg mL^{-1} Cd was reached employing the preconcentration step proposed, being almost 5-times better than in online mode without preconcentration step and with the same AAS detector (60 pg L^{-1} Cd). This method seems to be promising for sensitive determination of cadmium in various environmental matrices. Future experiments will focus on quantification of trapping capacity of the gold nanoparticles and evaluation of potential interferences.

References

[1] *IARC Monographs on the Evaluation of Carcinogenic Risk to Humans. Volume 58: Beryllium, Cadmium, Mercury, and Exposures in the Glass Manufacturing Industry.* International Agency for Research on Cancer 1993, p. 119–238.
[2] Sagapova L., Musil S., Kodríková B., Svoboda M., Kratzer J.: Effect of additives on cadmium chemical vapor generation and reliable quantification of generation efficiency. *Analytica Chimica Acta* **1168** (2021), 338601.

[3]　Migašová M., Matoušek T., Schrenková V., Žídek R., Petry-Podgórska I., Kratzer J.: Mercury volatile species generation from HCl and TRIS buffer media: Quantification of generation efficiency and characterization of severe changes in speciation information due to de-alkylation. *Analytica Chimica Acta* **1119** (2020), 68–76.

[4]　de Oliveira A.F., Svoboda M., Benada O., Kratzer J.: Ultratrace determination of arsenic by hydride generation atomic absorption spectrometry with preconcentration on gold nanoparticles. *Journal of Analytical Atomic Spectrometry* **37** (2022), 620–631.

[5]　de Oliveira A.F., Svoboda M., Musil S., Machado I., Vaněk D., Matoušek T., Dědina J., Kratzer J.: Selenium preconcentration in a gold "amalgamator" after hydride generation for atomic spectrometry. *Journal of Analytical Atomic Spectrometry* **35** (2020), 2132–2141.

[6]　Dědina J., Matoušek T.:Multiple microflame—a new approach to hydride atomization for atomic absorption spectrometry. *Journal of Analytical Atomic Spectrometry* **15** (2000), 301–304.

[7]　Matoušek T., Dědina J., Selecká A.: Multiple microflame quartz tube atomizer — further development towards the ideal hydride atomizer for atomic absorption spectrometry. *Spectrochimica Acta B* **57** (2002), 451–462.

Optimization of LC-MS method for the determination of food additives in popular food commodities

Aliaksandra Kharoshka[a, *], Aleš Krmela[a], Věra Schulzová[a], Jana Hajšlová[a]

[a] *Department of Food Analysis and Nutrition, Faculty of Food and Biochemical Technology, University of Chemistry and Technology Prague, Technická 3, 166 28 Prague 6, Czech Republic*
   ✉ *kharosha@vscht.cz*

Keywords
food additives
ketchup
LC-MS
optimization

Abstract
Food additives are compounds that are added to food for a specific technological purpose. To control the compliance with regulatory requirements, food additives must be quantitatively determined. The aims of this study were to come up with a fast and reproducible method for quantitative determination of 19 food additives and 5 compounds that can be added to foods but are not considered as additives in European Union. Different extraction conditions were tested to find what works the best for all analytes. Quantitative determination was done employing liquid chromatography with mass spectrometry (LC-MS). Due to observed matrix effects, analytical column and separation conditions were also optimized in order to achieve sufficient separation and great peak shapes. The optimized method was later validated providing with great recovery (80–112%) and repeatability values (5.6–13%).

1. Introduction

Food additives are defined as compounds that are added to food for a specific technological purpose, for example, texture modification, prolongation of the shelf life of a product or change of the product's appearance. In European Union usage of these substances is regulated by the Regulation (EC) No 1333/2008 [1]. Food additives are divided into 27 classes based on the application function. Application of food additives affects the product in different ways, it can lower the price or prolongate its shelf-life, which can minimize food waste. Moreover, usage of sweeteners provides an opportunity to consume sweet products for people suffering from diabetes. On the other hand, undeclared usage of some additives can result in unwanted health effects for consumers. Considering possible health problems as well food adulteration, food additives usage is highly controlled in European Union [2].

The first step in the determination of food additives is extraction. In case of liquid samples, usually only filtration and dilution are needed while solid samples may require sonication and multistep solvent extraction. Determination can be performed employing different techniques such as spectrophotometric methods, electroanalytical and electromigration techniques, and both liquid and gas chromatography coupled with conventional detectors or a mass spectrometer [3]. The choice depends on the chemical and physical properties of the analyte. For example, food colourants can be determined by spectrophotometry or thin layer chromatography [4]. However, because food colourants can be added in very small amounts, these instruments are not always capable of detecting them. Sweeteners can be reliably determined by gas chromatography coupled with mass spectrometry, but such analysis is time-consuming and requires complex sample manipulation [5]. In order to simultaneously determine as many compounds as possible, liquid chromatography coupled with mass spectrometry are often used [6]. As some additives are used at very low levels, both single and tandem mass spectrometers can be employed [7].

The aims of this study were to optimize existing extraction procedure as well as improve separation of the analytes. The sample matrix used for the experiments was ketchup that didn't contain any of the tested analytes and represented complex food matrix. Each tested procedure was validated, and repeatability was expressed as relative standard deviation (*RSD*, %, *n* = 6). The resulting analytical method can be applied for the quantitative determination of 19 food additives and 5 compounds that can be added or found in food and beverages.

2. Experimental

2.1 Reagents and chemicals

Analytical standards of tartrazine, sunset yellow FCF, azorubine, ponceau 4R, allura red AC, patent blue V calcium salt, brilliant blue FCF, brilliant black BN, green S, fluorescein, erythrosine B, sorbic acid, benzoic acid, sodium cyclamate, sodium saccharin, sucralose, neohesperidine dihydrochalcone, neotame, ethyl-vanillin, vanillin, and theobromine were purchased from Sigma Aldrich (Germany). Anhydrous caffeine and acesulfame K were purchased from Fluka (Germany), aspartame from Supelco (USA). HPLC-grade methanol was obtained from Sigma Aldrich (Germany). Analytical grade ammonium acetate was purchased from Sigma Aldrich (Germany). Water was purified using a Milli-Q Ultrapure water purification system from Millipore (USA).

2.2 Sample preparation

5 g of the sample is weighed to a plastic test tube, then 5 mL 20% methanol in water with pH adjusted using acetic acid or ammonia to values 3, 8 or 11 is added

to the test tube. The sample is shaken vigorously and ultrasonicated for 10 minutes. After centrifugation (10000 RPM, 5 minutes, 5 °C), the supernatant is collected in a 50 mL volumetric flask and the procedure is then repeated by adding 5 mL of the solvent. Extraction is performed 6–8 times depending on pH of the solvent. The resulting combined extract is filled up to 50 mL with extraction solvent in a volumetric flask. An aliquot of the solution is filtered through a PTFE centrifugal microfilter with a porosity of 0.22 μm and transferred to a vial. If necessary, the solution is further diluted with solvent.

2.3 Instrumentation

Waters Acquity UPLC iClass system (Waters, USA) was used for the separation with BEH C18 analytical column (100×2.1 mm, 1.7 μm, Waters, USA) which was later changed for Luna Omega Polar C18 (100×2.1 mm, 1.6 μm, Phenomenex, USA). For BEH C18 column the mobile phase consisted of 5 mM ammonium acetate aqueous solution (A) and methanol (B), gradient elution was used. Mobile phase flow rate was set at 0.4 mL/min. Column temperature was 60 °C. The injection volume was 3 μL. Separation on Luna Omega Polar C18 column was achieved using the same mobile phase and gradient elution. Mobile phase flow rate was set at 0.4 mL/min. Column temperature was 40 °C. The injection volume was 3 μL.

Detection was performed using a single quadrupole MS system (QDa, Waters, USA) with electrospray ionization (ESI). Acquisition and data processing were carried out using Masslynx v.4.1 software (Waters, USA). Identification was based on comparison of *m/z* values and retention times of the measured substances with the standards. Quantification was done using external calibration.

3. Results and discussion

This study was focused on the optimization of extraction and separation of food additives that represented synthetic colourants (10 authorized and 1 unauthorized), synthetic sweeteners (7), preservatives (2), flavourings (1 natural and 1 synthetic) and purine alkaloids (2) that can be added to food. In the first part of this study, extraction of analytes from solid samples was optimized. Selected compounds differ in physical and chemical behaviour; therefore, simultaneous extraction of all groups can be tricky. Ketchup was chosen as a sample because it is a compound-rich matrix. In order to perform the experiments, a sample of a ketchup that was free from any of the analytes, was contaminated with the mixed standard solution of all analytes. Each extraction procedure was examined in terms of time needed to perform extraction, recovery of the analytes and repeatability expressed as relative standard deviation (%). All procedures included ultrasonication step as well as repeated extraction with a new portion of the solvent. Based on the behaviour of the analytes, 20% methanol in water was

Table 1
Recovery and repeatability values of three tested extraction procedures (n.d. – not detected, values in bold are considered the best for the analyte).

	pH = 3		pH = 8		pH = 11	
	Recovery/%	*RSD*/%	Recovery/%	*RSD*/%	Recovery/%	*RSD*/%
Colorants						
Fluorescein	81.3	7.6	96.2	12.6	**100.1**	**9.3**
Brilliant Blue	48.6	7.6	93.8	10.6	**92.1**	**5.5**
Allura Red	43.1	7.0	105.2	6.6	**98.8**	**5.5**
Erythrosine	n.d.	n.d.	80.1	8.4	**98.6**	**8.0**
Patent Blue	100.6	7.9	97.8	10.1	**101.2**	**6.7**
Tartrazine	70.0	5.9	112.1	11.4	**107.3**	**7.9**
Green S	82.6	5.8	**90.6**	**9.1**	36.1	5.4
Ponceau 4R	36.9	8.7	110.7	11.1	**92.5**	**3.8**
Sunset Yellow	74.9	4.6	94.4	8.3	**89.6**	**2.8**
Azorubine	20.2	7.3	89.1	7.8	**98.0**	**6.7**
Brilliant Black BN	56.6	9.2	85.4	10.8	**94.8**	**3.3**
Sweeteners						
Aspartame	**97.0**	**7.8**	86.8	13.2	6.1	9.5
Neotame	**102.4**	**3.2**	107.8	7.5	8.2	15.9
Cyclamate	**104.2**	**1.4**	108.3	10.2	104.4	3.2
Saccharin	n.d.	n.d.	**97.8**	**8.4**	103.2	8.5
Neohesperidine DC	**104.6**	**3.1**	93.5	13.0	37.7	8.7
Sucralose	**104.4**	**5.9**	98.6	5.6	103.4	5.5
Acesulfame K	**99.6**	**8.8**	97.4	10.6	100.7	9.4
Preservatives						
Sorbic acid	**110.7**	**4.3**	92.2	11.7	102.0	9.3
Benzoic acid	**97.5**	**6.0**	93.1	9.0	101.1	7.6
Others						
Ethylvanillin	**93.8**	**5.2**	96.9	10.3	95.6	7.4
Theobromine	**94.2**	**5.8**	101.9	12.6	109.8	9.1
Caffeine	71.3	4.4	88.9	9.4	**110.5**	**5.0**
Vanillin	**98.8**	**1.4**	99.2	8.1	98.8	3.0

chosen for the extraction which was later modified with acetic acid or ammonia to create acidic (pH = 3), neutral (pH = 8), and basic conditions (pH = 11). These experiments showed that all analytes can be extracted with neutral 20% methanol (pH = 8). However, this extraction procedure was more time-consuming and resulted in 8 repetitions of the extraction needed to ensure the best extractability of the analytes, obtained RSD values were up to 13%. When acidic extraction was tested, colourants, except for green S and patent blue, were only partially extracted from the sample but the rest of the analytes had very good recovery values. This procedure resulted in 6 repeated extractions and RSD values lower than 10%. The last tested condition was basic extraction that was great for the
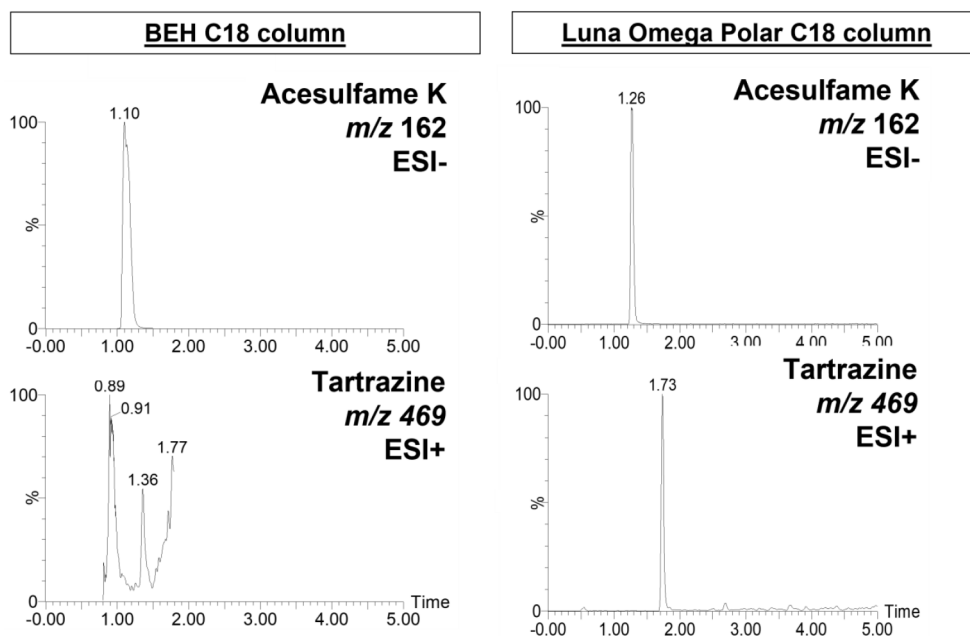
Fig. 1 XIC chromatograms of acesulfame K and tartrazine in ketchup obtained using BEH C18 and Luna Omega Polar C18 columns

extraction of almost all compounds except for sweeteners aspartame, neotame and neohesperidine dihydrochalcone. It also needed 6 repeated extractions to obtain the highest recovery values and repeatability was lower than 10%. Based on the obtained information, neutral extraction was chosen as the best one as it resulted in simultaneous extraction of all analytes with recovery values in range of 80-112% and RSD values from 5.6 to 13%. Results of all tested procedures are summed up in Table 1.

The second part of the optimization was related to separation of the analytes. When ketchup was used as a sample matrix, unwanted matrix effects were observed. To achieve better peak shape and to prolong retention times of the analytes that are eluted close to the dead volume of the column, another reverse phase column was tested. Mobile phase composition remained the same, but gradient and temperature were optimized using mixed standard solution. After the optimizations, measurement of the same extracts using BEH C18 and Luna Omega Polar C18 was performed. Based on the obtained chromatograms, it was obvious that Luna Omega Polar C18 was better for the determination of the selected food additives. XIC chromatograms of analytes acesulfame K and tartrazine in contaminated ketchup are shown in Fig. 1.

4. Conclusions

This study was centred on the optimization of extraction procedure and liquid chromatography conditions such used column, elution gradient and column temperature for the quantitative determination of 24 analytes that represent different classes of compounds that can be added to food. Effect of pH was tested for different groups of food additives. Optimized method was validated and provided with acceptable recovery (80–112%) and great *RSD* values (5.6–13%). This method can be further used for the quantitative determination of 24 compounds in solid samples such as jams, spices, sweets, etc.

Acknowledgments

References

[1]   http://data.europa.eu/eli/reg/2008/1333/oj (accessed 25th June 2022)
[2]   Debeuckelaere W.: Legislation on food additives, food enzymes and flavourings in the European Union. *Current Opinion in Food Science* **6** (2015), 49–52.
[3]   Martins F.C., Sentanin M.A., De Souza D.: Analytical methods in food additives determination: Compounds with functional applications. *Food Chemistry* **272** (2019), 732–750.
[4]   Rejczak T., Tuzimski T.: Application of high-performance liquid chromatography with diode array detector for simultaneous determination of 11 synthetic dyes in selected beverages and foodstuffs. *Food Analytical Methods* **10** (2017), 3572–3588.
[5]   Zygler A., Wasik A., Namieśnik J.: Analytical methodologies for determination of artificial sweeteners in foodstuffs. *TrAC Trends in Analytical Chemistry* **28** (2009), 1082–1102.
[6]   Krmela A., Kharoshka A., Schulzova V., Pulkrabova J., Hajslova J.: A simple LC–MS multi-analyte method to determine food additives and caffeine in beverages. *LCGC Europe* **33** (2020), 327–335.
[7]   Martin F., Oberson J.M., Meschiari M., Munari C.: Determination of 18 water-soluble artificial dyes by LC–MS in selected matrices. *Food Chemistry* **197** (2016), 1249–1255.

GC-MS identification of photochemically generated volatile species of tungsten

Jaromír Vyhnanovský[a, b, *], Sándor T. Forczek[c], Stanislav Musil[a]

[a] *Institute of Analytical Chemistry of the Czech Academy of Sciences, Veveří 97, 602 00 Brno, Czech Republic ✉ jaromir.vyhnanovsky@gmail.com*
[b] *Department of Analytical Chemistry, Faculty of Science, Charles University, Hlavova 8/2030, 128 43 Prague 2, Czech Republic*
[c] *Institute of Experimental Botany of the Czech Academy of Sciences, Vídeňská 1083, 142 20 Prague 4, Czech Republic*

Keywords
gas chromatography mass spectrometry
photochemical vapor generation
tungsten

Abstract
The volatile product of photochemical vapor generation of tungsten has been identified by GC-MS for the first time. A 19 W thin-film flow-through UV photoreactor was employed and the volatile species of tungsten was generated from a formic acid based medium in the presence of cadmium ions as a sensitizer. The gas phase containing argon as a carrier gas was sampled by a syringe from a gas-liquid separator and examined by GC-MS. Tungsten hexacarbonyl was clearly identified in the gas phase while attempts to identify products of photochemical vapor generation of other elements (namely Ru and Re) were unsuccessful probably due to their low stability.

1. Introduction

Photochemical vapor generation, a sample introduction technique for analytical atomic spectrometry, has been slowly earning its place amongst other more mature vapor generation techniques such as hydride generation. It employs a source of UV-radiation that irradiates (most commonly) a low molecular weight organic acid containing medium with an analyte. Highly reducing radicals and aquated electrons are produced and convert the analyte into a volatile species which is then transported into a detector [1].

The usability of photochemical vapor generation has already been described for some 30 elements spanning hydride-forming elements [2, 3], transition metals [4–9] and even non-metals [10–11], and this number keeps growing each year. But this pursue of adding new elements to a growing list has overshadowed the fundamental aspects of photochemical vapor generation, leaving much to be desired regarding the understanding of the mechanisms behind photochemical vapor generation.
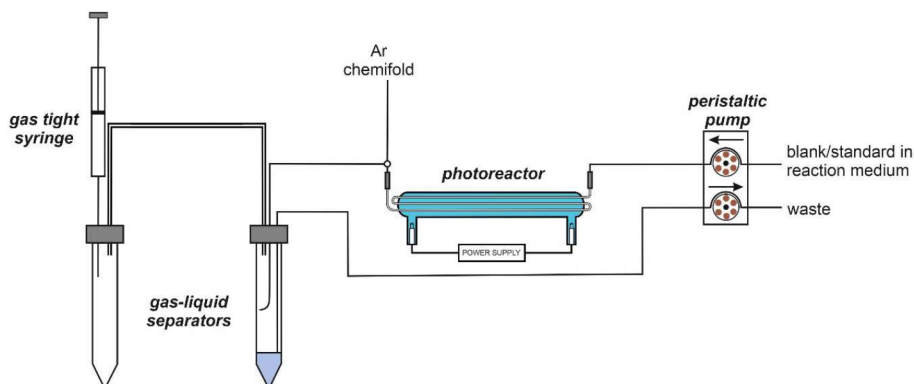
Fig. 1 Schematic diagram of a photochemical vapor generation system with sampling of the gas phase for GC-MS identification.

Knowing the identity of the generated products is a first step in the direction towards proposal of a mechanism of photochemical vapor generation, and while the volatile products of many elements have already been identified by GC-MS and some have been speculated and discussed, the identity of others is still a mystery [12].

In this work, we provide GC-MS identification of $W(CO)_6$ as the stable product of photochemical vapor generation of W(VI) generated from a solution of formic acid in the presence of Cd ions [6].

2. Experimental

2.1 Reagents and chemicals

Deionized water ($<0.2\,\mu S\,cm^{-1}$, Ultrapur, Watrex, USA) was used for preparation of all solutions. Formic acid (98%, p.a., Lach-Ner, Czech Republic) was used for the preparation of the reaction medium. Stock standard solutions of $1000\,mg\,L^{-1}$ W in 2% KOH was obtained from Aldrich (USA). Cadmium(II) acetate dihydrate (p.a., Lach-Ner, Czech Republic) was used for the preparation of a sensitizer stock solution. Solid tungsten hexacarbonyl (97%, Sigma-Aldrich, USA) was used for method development and as a GC-MS standard. Liquid iron pentacarbonyl (purum, Fluka AG, Germany) was used in the preliminary experiments.

2.2 Instrumentation

A schematic diagram of the photochemical vapor generation system in a continuous flow mode is shown in Fig. 1 and is very similar to the one in [6]. All tubing used was made from PTFE except for tygon tubing in the peristaltic pump (Reglo ICC, Ismatec, Switzerland). A thin-film flow-through photoreactor was a 19 W low-pressure mercury discharge lamp (Beijing Titan Instruments, China)

with a quartz channel (≈720 µL internal volume) immersed in the discharge. While continuously irradiating a solution of W(VI) in a medium of 40% (*v/v*) HCOOH containing $500\,mg\,L^{-1}$ Cd(II) at $2\,mL\,min^{-1}$, the effluent from the photoreactor and the generated volatile species were carried by $100\,mL\,min^{-1}$ of Ar(chemifold) into two similar gas-liquid separators connected in series (internal volume 15 mL). In the first separator, the volatile species were separated from the liquid phase while the second one allowed for convenient sampling of the gas phase containing volatile species. A set volume of the gas phase was manually withdrawn with a gas tight syringe (Hamilton, USA) and immediately injected into a Varian 240-MS GC-MS (Agilent Technologies, USA) fitted with a 15 m Rxi-5ms column (5% diphenyl/95% dimethyl polysiloxane, 0.32 mm i.d. × 1.0 µm film, Restek, USA). Operating conditions were as follows: 200 °C injection port temperature with an oven program initially at 75 °C for a period of 3.0 min followed by a 65 °C min^{-1} ramp to 270 °C and hold for 0.5 min at a He flow rate of $1.0\,mL\,min^{-1}$. Detection was performed in full scan mode *m/z* 50–400; the mass spectrometer detector was operated in electron ionization mode at 70 eV and auto-tuned prior to analyses. Solid phase microextraction (SPME) by means of a Divinylbenzene/Carboxen/-Polydimethylsiloxane fiber (Supelco grey, Sigma-Aldrich, USA) was used to preconcentrate analyte from the gas phase to enhance detection capability.

3. Results and discussion

Preliminary experiments and method development for GC-MS identification were performed using a liquid $Fe(CO)_5$ that was placed into a gas tight vial with a septum and let to reach an equilibrium between the liquid and gas phase. Different volumes of the gas phase containing $Fe(CO)_5$ sampled from the headspace were tested and GC program and MS instrument parameters optimized in order to obtain as high MS peak intensity as possible. Similarly, the feasibility of SPME preconcentration was tested using different types of SPME fibres and preconcentration times.

Subsequently, a gas phase in the vial containing solid $W(CO)_6$ (suspected volatile product of photochemical vapor generation of tungsten) was examined using the conditions found optimal for detection of $Fe(CO)_5$ in order to find the retention time and isotopic and fragmentation pattern of $W(CO)_6$. The feasibility of SPME preconcentration was tested for $W(CO)_6$ as well.

Using optimal generation conditions described in our previous work [6], the unknown volatile product of photochemical vapor generation of tungsten was sampled from the second gas-liquid separator of the generator (Fig. 1) and examined by GC-MS. Again, various parameters of the generator (especially Ar chemifold flow rates) as well as W(VI) concentration used for photochemical vapor generation had to be optimized to obtain as high MS peak intensity as possible and clear mass spectra.
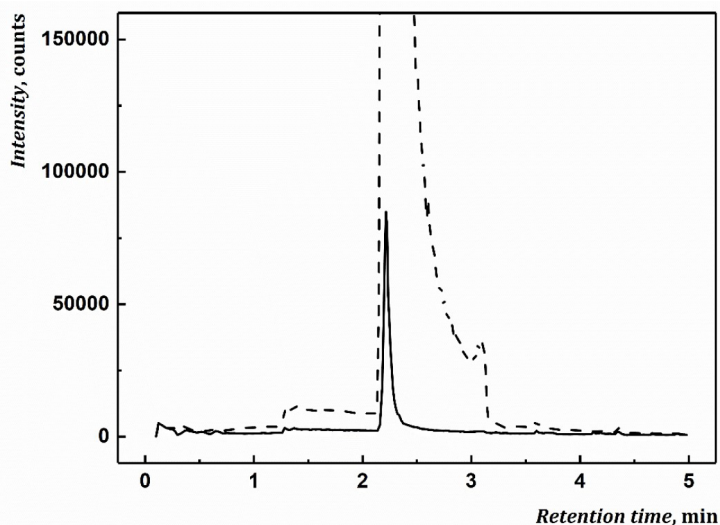
Fig. 2 Total ion chromatograms (full scan mode, m/z 50–400) generated following: (dash line) gas sampling of the headspace above a room temperature solid sample of $W(CO)_6$ and (solid line) that from the effluent during continuous photolysis of 5 mg L^{-1} W(VI) in a medium comprising 40% (v/v) HCOOH and 500 mg L^{-1} Cd(II).
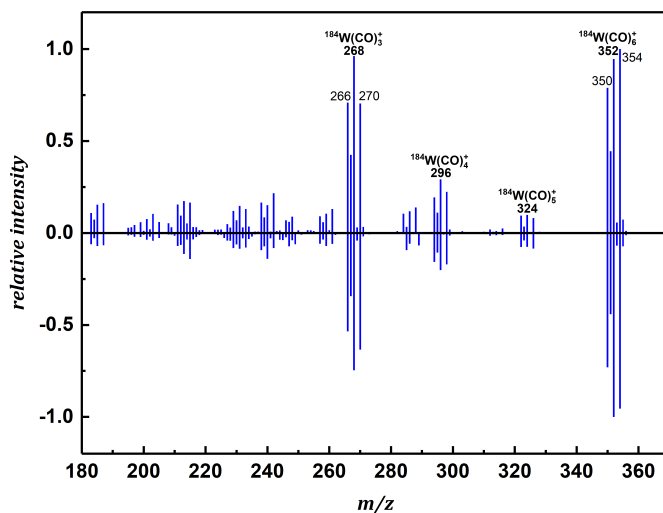

Fig. 3 Mass spectra of: (upper display) $W(CO)_6$ following gas sampling of the gas phase arising from continuous photochemical vapor generation of 5 mg L^{-1} W(VI) from a medium comprising 40% (v/v) HCOOH and 500 mg L^{-1} Cd(II); and (lower display) from gas sampling of the headspace above a solid standard of $W(CO)_6$.

Chromatograms of the unknown volatile tungsten species and the known standard of solid $W(CO)_6$ are compared in Fig. 2. It is clearly evident that both of these compounds have very similar retention times and patterns. Fig. 3 shows the respective mass spectra sampled from both the photochemical vapor generation system and the headspace above the solid standard. Again, a close match in fragmentation and isotopic patterns of these two spectra is visible, and both spectra match that of $W(CO)_6$ available in the NIST MS database [13]. While some significant differences in the three spectra can be observed, these can be attributed to the quite complicated composition of the gas phase exiting the generator (mainly Ar but also significant amounts of CO, CO_2 and formic acid vapors) and other unknown experimental artifacts. Nevertheless, the close match in the isotopic and fragmentation patterns of the unknown product and $W(CO)_6$ standard, as well as a close match to the NIST MS spectra, is a very strong evidence that the unknown tungsten compound produced by photochemical vapor generation is, in fact, $W(CO)_6$, as was presumed earlier [6]. Continuous sampling of the gas phase for a period of 25 min by SPME provided a 600-fold increase in MS peak intensities due to the resulting preconcentration of $W(CO)_6$ in the second gas-liquid separator.

The identification of the unknown photochemically generated compounds of Ru [14] and Re [15] was, however, unsuccessful probably due to their lower thermal stability and/or higher reactivity. Use of SPME to preconcentrate the species prior to GC-MS also did not prove fruitful.

4. Conclusions

For the first time ever, irrefutable GC-MS evidence has been provided to confirm that the product of photochemical vapor generation of tungsten is $W(CO)_6$. A similar effort was made for the products of photochemical vapor generation of ruthenium and rhenium, but both were unsuccessful, which suggests a lower thermal stability or higher reactivity of these species. Other, more direct approaches such as Direct Analysis in Real Time (DART)-MS may be more suitable for the identification of such compounds.

References

[1]   Sturgeon R.E.: Photochemical vapor generation: a radical approach to analyte introduction for atomic spectrometry. *Journal of Analytical Atomic Spectrometry* **32** (2017), 2319–2340.
[2]   Vyhnanovský J., Yildiz D., Štádlerová B., Musil S.: Efficient photochemical vapor generation of bismuth using a coiled Teflon reactor: Effect of metal sensitizers and analytical performance with flame-in-gas-shield atomizer and atomic fluorescence spectrometry. *Microchemical Journal* **164** (2021), 105997.

[3]   Zheng C., Ma Q., Wu L., Hou X., Sturgeon R.E.: UV photochemical vapor generation–atomic fluorescence spectrometric determination of conventional hydride generation elements, *Microchemical Journal* **95** (2010), 32–37.
[4]   Šoukal J., Sturgeon R.E., Musil S.: Efficient photochemical vapor generation of molybdenum for ICPMS detection. *Analytical Chemistry* **90** (2018), 11688–11695.
[5]   de Oliveira R.M., Borges D.L.G.: UV photochemical vapor generation of noble metals (Au, Ir, Pd, Pt and Rh): A feasibility study using inductively coupled plasma mass spectrometry and seawater as a test matrix. *Journal of Analytical Atomic Spectrometry* **33** (2018), 1700–1706.
[6]   Vyhnanovský J., Sturgeon R.E., Musil S.: Cadmium assisted photochemical vapor generation of tungsten for ICPMS detection. *Analytical Chemistry* **91** (2019), 13306–13312.
[7]   Guo X., Sturgeon R.E., Mester Z., Gardner G.J.: Vapor generation by UV irradiation for sample introduction with atomic spectrometry. *Analytical Chemistry* **76** (2004), 2401–2405.
[8]   Nováková E., Horová K., Červený V., Hraníček J., Musil S.: UV photochemical vapor generation of Cd from a formic acid based medium: optimization, efficiency and interferences. *Journal of Analytical Atomic Spectrometry* **35** (2020), 1380–1388.
[9]   Šoukal J., Musil S.: Detailed evaluation of conditions of photochemical vapor generation for sensitive determination of nickel in water samples by ICP-MS detection. *Microchemical Journal* **172** (2022), 106963.
[10]   Hu J., Sturgeon R.E., Nadeau K., Hou X., Zheng C., Yang L.: Copper ion assisted photochemical vapor generation of chlorine for its sensitive determination by sector field inductively coupled plasma mass spectrometry. *Analytical Chemistry* **90** (2018), 4112–4118.
[11]   Grinberg P., Sturgeon R.E.: Ultra-trace determination of iodine in sediments and biological material using UV photochemical generation-inductively coupled plasma mass spectrometry. *Spectrochimica Acta Part B: Atomic Spectroscopy* **64** (2009), 235–241.
[12]   Pagliano E., Vyhnanovský J., Musil S., de Oliveira R.M., Forczek S.T., Sturgeon R.E.: GC-MS exploration of photochemically generated species of Os, W and Ru from reductive and oxidative media. *Journal of Analytical Atomic Spectrometry* **37** (2022), 528–534.
[13]   https://webbook.nist.gov/cgi/cbook.cgi?ID=C14040110. Accessed on 23.6.2022
[14]   Musil S., Vyhnanovský J., Sturgeon R.E.: Ultrasensitive detection of ruthenium by coupling cobalt and cadmium ion-assisted photochemical vapor generation to inductively coupled plasma mass spectrometry. *Analytical Chemistry* **93** (2021), 16543–16551.
[15]   Vyhnanovský J., Hašlová K., Musil S.: Novel photochemical vapor generation of rhenium for its ultratrace determination. In: *Proceedings of the 17th ISC Modern Analytical Chemistry*. K. Nesměrák (ed.). Prague, Faculty of Science, Charles University 2021, p. 200–204.

Study of meconium sample pretreatment for the determination of plasticizer DINCH metabolites by HPLC-MS/MS

Lucia Vráblová[a],[*], Zuzana Široká[a], Helena Jurdáková[a], Renáta Górová[a]

[a] *Department of Analytical Chemistry, Faculty of Natural Sciences, Comenius University, Ilkovičova 6, 842 15 Bratislava, Slovakia* ✉ *lucia.vrablova26@gmail.com*

Abstract
The topic of environmental health is currently very actual and, in order to minimise people's exposure to harmful substances from the environment, these are replaced by less harmful substances from the environment. Such an example is the replacement of harmful phthalates used to soften plastics with a new DINCH plasticizer, which was put into use since 2002 after favourable results of toxicological tests. In this paper, we optimised the method for meconium analysing by high-performance liquid chromatography coupled with tandem mass spectrometry (HPLC-MS/MS). Matrix as meconium is suitable for the assessment of prenatal exposure. The aim was the study of meconium sample pretreatment using various solvent extraction procedures with subsequent determination by HPLC-MS/MS.

1. Introduction

At present, great emphasis is placed on environmental health, i.e., the environmental-health relationship. It is the task of human biomonitoring to assess the extent to which the organism is exposed to environmental contaminants. Analyses of human tissues and biological fluids shall be carried out within human biomonitoring, considering all possible pathways and relevant sources of exposure. The European Programme for Human Biomonitoring has identified plasticizers as substances of priority interest [1]. Plasticizers are used to soften plastic materials, e.g., in the manufacture of toys, floor coverings, food packaging or medical devices.

Among the most widely used plasticizers in the past were phthalates *di*(2-ethylhexyl)phthalate and *di*-izononyl phthalate, which have been due to their adverse health effects (renal toxicity, endocrine disruptors) [2] gradually replaced by Hexamoll® DINCH plasticizer (cyclohexyl acid diisononyl ester-1,2-dicarboxyl acid) since 2002 [1]. The specific biomarkers of DINCH exposure are three oxidative products of cyclohexane-1,2-dicarboxylic acid: mono(hydroxyiso-
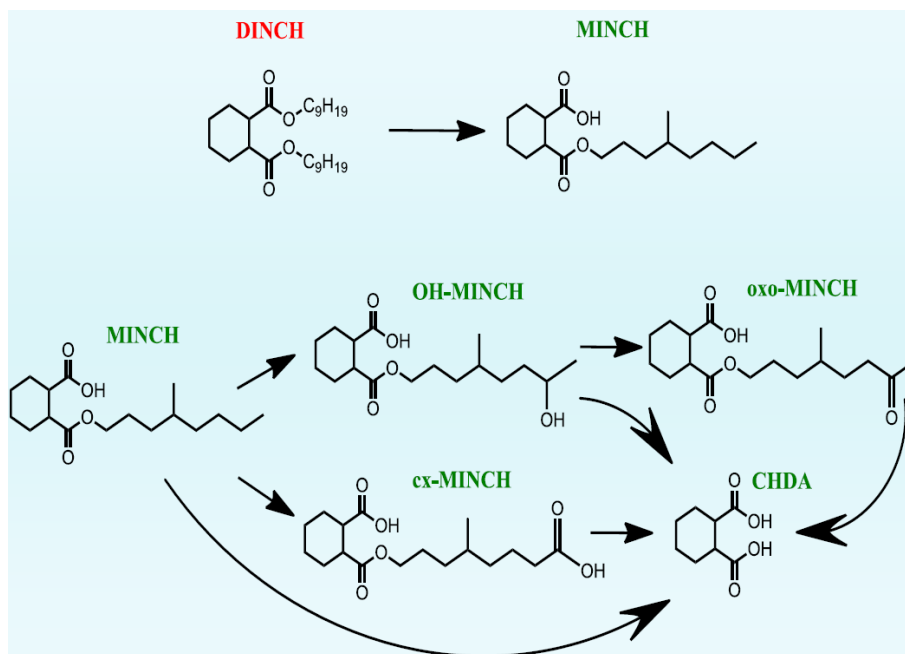
Fig. 1 Metabolism of di-isononyl-phthalate (DNCH): mono-isononyl-cyclohexane-1,2-dicarboxylate (MINCH), mono(hydroxyisononyl)ester (OH-MINCH), mono(carboxyisooctyl)ester (cx-MINCH), mono(oxoisononyl)ester (oxo-MINCH), and cyclohexane-1,2-dicarboxylic acid (CHDA)

nonyl)ester (OH-MINCH), mono(carboxyisooctyl)ester (cx-MINCH) and mono-(oxoisononyl)ester (Fig. 1). As consumption as well as exposure to this plasticizer is increasing, in addition to monitoring those biomarkers and DINCH compounds in urine, it is therefore appropriate to determine them in other matrices used for human biomonitoring.

Meconium is the first stool of newborn with a semi-solid consistency. It is black-green in colour and mostly odourless. It is composed of epithelial tissues, amniotic fluid, mucus, bile pigments and water. Meconium testing is non-invasive and allows prenatal exposure to be detected from approximately the 12–13th week of pregnancy, when the meconium begins to accumulate in the foetus, but its excretion occurs only after birth. Thus, the concentration of xenobiotic markers in the meconium represents the cumulative exposure during pregnancy [3]. The analytes identified in meconium include alcohol metabolites, illicit drugs, medicines, heavy metals, organic pollutants and their metabolites, neurotoxic substances and other xenobiotics [4]. Since meconium is a rather complex matrix, several pretreatment techniques need to be used before the analysis itself [5]. The whole process can often takes several hours. The two basic strategies for the isolation of analytes from the sample include solvent as extraction medium and the use of solid sorbent (SPE). Ultrasonic, microwave or Soxlet extraction is also often used to increase extraction efficiency [3].

Table 1
Quantification SRM transitions for studied analytes: mono(carboxyisooctyl)ester (cx-MINCH), and mono(hydroxyisononyl)ester (OH-MINCH), and their deuterated analogs.

Analyte	Precursor m/z	Product m/z	Collision energy/ V	Lens voltage /V
cx-MINCH	327.2	173.1	17	72
OH-MINCH	313.2	153.1	17	70
D8-cx-MINCH	335.2	173.1	16	70
D8-OH-MINCH	321.2	161.1	17	73

This work was focused on the study of meconium sample pretreatment for the determination of oxidised metabolites of the DINCH plasticizer using the HPLC-MS/MS method with the potential for biomonitoring studies and for the evaluation of human exposure to this substance in the prenatal development period.

2. Experimental

2.1 Reagents and chemicals

Mono(carboxyisooctyl)ester, mono(hydroxyisononyl)ester and their deuterated analogs (TRC, Canada). Methanol, deionised water, acetonitrile of LC-MS grade, and ethyl acetate (Fisher Scientific Chemicals, UK). *n*-Hexane and acetic acid (Mikrochem, Slovakia). Ammonium acetate and β-glucuronidase (Merck, Germany), meconium from anonymous donors.

2.2 Instrumentation

The analysis was performed in a reversed-phase HPLC system with C18 stationary phase using liquid chromatograph Dionex UltiMate 3000 RS. The mobile phase was water with 0.05% acetic acid (A) and acetonitrile with 0.05% acetic acid (B) at a flow rate of 0.23 mL/min and gradient elution from 90% A to 100% B in 15 min, then 3 min hold. The injection volume was 210 μL. TSQ mass spectrometer (Thermo Fisher Scientific) with triple quadrupole as analyzer scanned in negative mode by SRM scan. Heated electrospray ionization was used as the ionization technique, with a capillary voltage of 2500 V, an evaporation temperature of 144 °C and a capillary temperature of 325 °C. The nitrogen flow rate of sheath gas, auxilliary gas and sweep gas was 4.2 L/min, 8 L/min and 1.5 L/min, respectively. The argon pressure in the collision cell was 1.5 mTorr. The quantification transitions for each analyte are shown in Table 1.

2.3 Meconium pretreatment

Samples spiked with analytes and isotope-labeled standards (D8-cx-MINCH and D8-OH-MINCH) were analyzed. The meconium sample was mechanically homogenised by mixing and weighed into a micro-test tube by metal spatula. DINCH metabolites are present in meconium in the form of glucuronide conjugates and therefore an important step in the pretreatment is the deconjugation process by enzyme β-glucuronidase. Ammonium acetate buffer (pH = 6, 200 μl) was added to the meconium, followed by addition of enzyme β-glucuronidase diluted with buffer (1:1) and the entire contents were mixed on a vortex and shaker (1500 rpm/25 min) to ensure homogenity. The samples were placed in a water bath for 3 h (37 °C). The reaction was stopped by adding 10 μL acetic acid and mixing on vortex, followed by centrifugation (35 min, 13 900 rpm). Subsequently, the extraction reagent ethyl acetate or ethyl acetate:hexane mixture was added and the samples were shaken on a shaker (1h/13 900 rpm). After centrifugation the top layer extract was collected on a filter plate, centrifuged for 5 min at 4600 rpm, the filtered extract was collected in a microtiter plate which was placed in the centrifuge under the titration plate, evaporated to dryness by a stream of air and reconstituted in a reconstitution solution (10% methanol in water, 0.05% acetic acid in water).

To evaluate the matrix effect, extraction recovery, and overall sample treatment efficiency, we prepared three types of samples. Standard enriched sample before extraction (sample A) to which standards were added at the beginning of the treatment process. The sample enriched with standard after extraction (sample B) and sample which consisted only of standards and reconstitution solution (sample C) [6].

Matrix effect (%) was evaluated using the equation

$$ME = 100 - 100\,(B/A) \tag{1}$$

where A is the average peak area of the standard in pure solvent, and B is the average peak area of the enriched extract after treatment.

Recovery (%) was evaluated using the equation

$$RE = 100\,(C/B) \tag{2}$$

Where C is the average peak area of the enriched extract before treatment.

And finally efficiency of the treatment process (%) was evaluated using the equation

$$PE = 100\,(C/A) \tag{3}$$

Table 2

Calculated parameters of supernatant and residue of meconium extraction with ethylacetate: mono(carboxyisooctyl)ester (cx-MINCH), mono(hydroxyisononyl)ester (OH-MINCH).

Parameter	cx-MINCH		OH-MINCH	
	Supernatant	Residue	Supernatant	Residue
Matrix effect / %	85	93	87	95
Recovery /%	25	30	22	32
Efficiency of the treatment process /%	3.8	2.1	2.9	1.6

3. Results and discussion

The values of matrix effect, recovery and overall process efficiency of the meconium sample treatment process were compared using extraction with ethyl acetate and ethyl acetate:hexane mixture in the ratios of 75:25, 50:50 and 25:75 as extraction reagents, respectively.

The first tested extraction reagent was ethyl acetate. Standards were added to the meconium sample at a concentration level corresponding to 60 ng/g meconium for cx-MINCH and OH-MINCH and 66.7 ng/g in meconium for their labelled standards. After deconjugation and centrifugation, the sample was separated into a supernatant and a solid residue, which were extracted separately with ethyl acetate. Table 2 shows the results for this tested sample treatment. The matrix effect for both cx-MINCH and OH-MINCH was highly significant at the 90% level, slightly lower for the supernatant than the residue. The extraction recovery is approximately 25–30% for both fractions. In case of ethyl acetate extraction of whole sample volume, recovery was almost 50% (Fig. 2). The overall efficiency for these procedures was low, at a few percent, mainly due to matrix effect.

Further extraction experiments were carried out with the ethyl acetate:hexane mixtures as extraction reagents in the ratios 25:75, 50:50 and 75:25 (Fig. 2). We found out the recoveries of the studied analytes varied in the range of 30–50% with the composition of the extraction reagent, increasing the hexane content in the extraction reagent significantly reduced the matrix effect and increased the overall efficiency of the procedure from about 3% for ethyl acetate to 47% for cx-MINCH and 36% for OH-MINCH for 25:75 mixture of ethyl acetate:hexane. In addition, the ethyl acetate extracts and also the extracts in the ethyl acetate:hexane 75:25 mixture were worse separated and in variable volumes after centrifugation and were slightly turbid. Extracts using ethyl acetate:hexane 50:50 and 25:75 mixtures were clear and a well-defined volumes could be taken (Fig. 3).
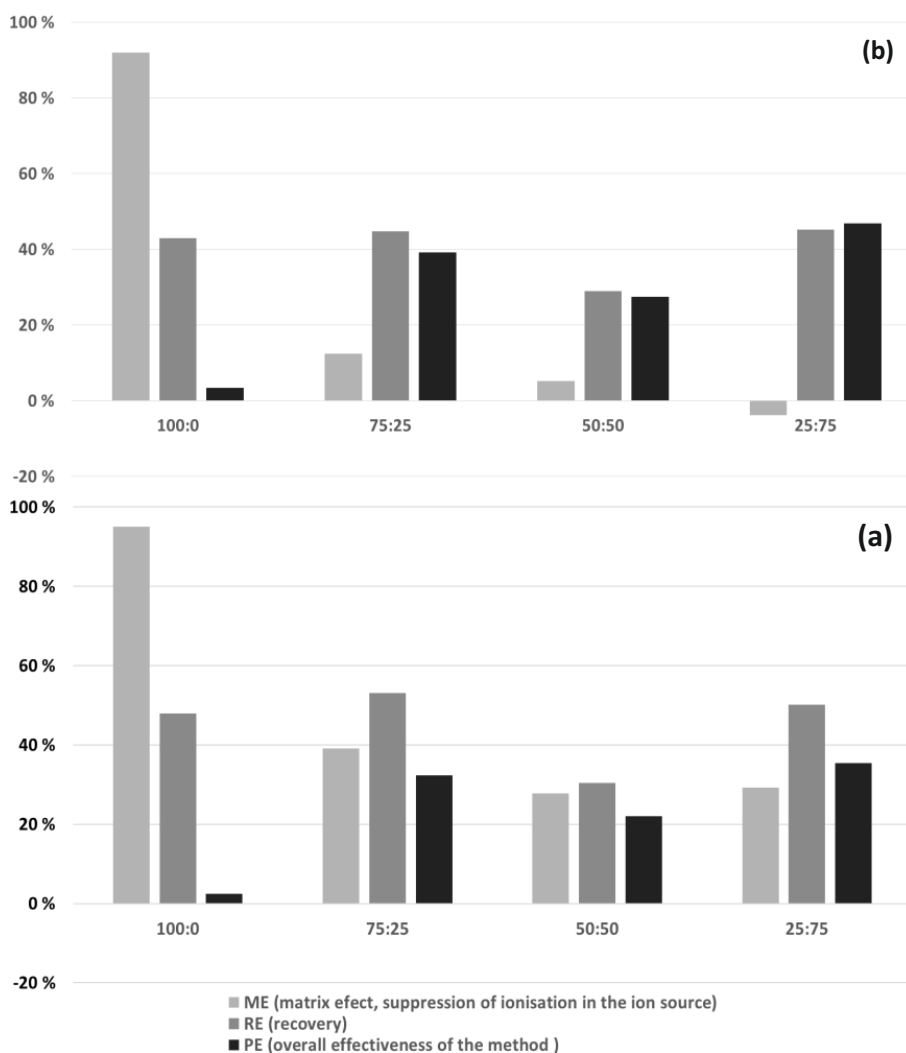
Fig. 2 Matrix effect, recovery and overall efficiency of the meconium sample treatment procedure for different extraction reagent compositions: (a) mono(hydroxyisononyl)ester (OH-MINCH), and (b) mono(carboxyisooctyl)ester (cx-MINCH).
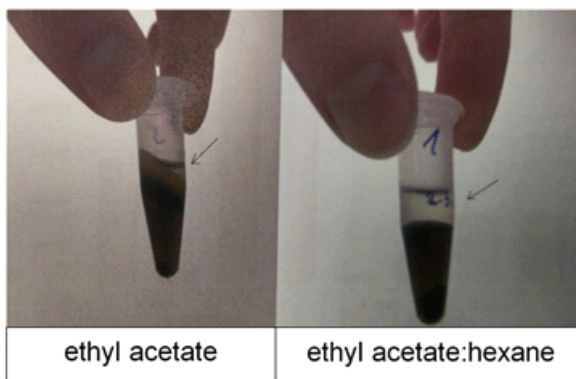

Fig. 3 Comparison of meconium sample volume extracts for ethyl acetate and ethyl acetate:hexane mixture (1:1).

Table 3

Calculated parameters for repetitive extraction of the meconium with 50:50 ethyl acetate:hexane mixture mono(carboxyisooctyl)ester (cx-MINCH), and mono(hydroxyisononyl)ester (OH-MINCH).

Parameter	cx-MINCH		OH-MINCH	
	1st extraction	2nd extraction	1st extraction	2nd extractinon
Matrix effect / %	−13	7	6	28
Recovery /%	42	6	33	4
Efficiency of the treatment process /%	47	6	31	3

The extraction with a mixture of ethyl acetate:hexane (50:50) was examined also in two consecutive steps, but the 2nd extraction did not bring any improvement (Table 3). The best overall efficiency and repeatability of the procedure was found out for the extraction with a 25:75 ethyl acetate:hexane mixture, but the values for both analytes were still below 50%.

4. Conclusions

Although the plasticizer DINCH and its metabolites are considered relatively safe, there is a need to continuously monitor their exposure in the human body. The meconium matrix is the subject of interest for biomonitoring studies of prenatal exposure. As it is a complex matrix, the disadvantage lies in the need for several treatment techniques. An important step in the analysis of meconium by HPLC-MS/MS is the optimization of the pretreatment process. We aimed at solvent extraction technique and our results have showed as the most suitable extraction reagent ethyl acetate:hexane in a ratio of 25:75. Optimization of the method requires further experiments.

References

[1] Kasper-Sonnenberg M., Koch H.M., Apel P., Ruther M., Palmke C., Bruning T., Kolossa-Gehring M.: Biomonitoring data on young adults from the Environmental Specimen Bank (ESB). *International Journal of Hygiene and Environmental Health* **222** (2019), 1084–1092.

[2] Directive 2005/84/EC of the European Parliament and the Council. *Official Journal of the European Union* **344** (2005), 40–3.

[3] Wózniak M.K., Jaszczak, E., Wiergowski M., Polkowska Z., Namieśnik, J., Biziuk M.: Meconium analysis as a promising diagnostic tool for monitoring fetal exposure to toxic substances: recent trends and perspectives. *TrAC Trends in Analytical Chemistry* **109** (2018), 124–141.

[4] Gareri J., Klein J., Koren G.: Drugs of abuse testing in meconium. *Clinica Chimica Acta* **366** (2006), 101–111.

[5]　　Moore Ch., Negrusz A., Lewis D.: Determination of drugs of abuse in meconium. *Journal of Chromatography B* **713** (1998), 137–146.

[6]　　Bienvenu J.F., Provencher G., Bélanger P. Bérubé R., Dumas P., Gagné S., Gaudreau É., Fleury N.: Standardized procedure for the simultaneous determination of the matrix effect, recovery, process efficiency, and internal standard association. *Analytical Chemistry* **89** (2017), 7560–7568.

Using HPLC-HRMS for identification of degradation products of selected azo dye

Lucia Hojová[a, *], Gabriela Kuchtová[b], Marian Vojs[c], Libor Dušek[b],
Andrea Vojs Staňová[a, d]

[a] *Department of Analytical Chemistry, Faculty of Natural Sciences, Comenius University in Bratislava, Mlynská Dolina, Ilkovičova 6, 842 15 Bratislava, Slovak Republic ✉ hojova4@uniba.sk*
[b] *Institute of Environmental and Chemical Engineering, Faculty of Chemical Technology, University of Pardubice, Studentská 573, 532 10 Pardubice, Czech Republic*
[c] *Institute of Electronics and Photonics, Faculty of Electrical Engineering and Information Technology, Slovak University of Technology in Bratislava, Ilkovičova 3, 812 19 Bratislava, Slovak Republic*
[d] *Research Institute of Fish Culture and Hydrobiology, South Bohemian Research Center of Aquaculture and Biodiversity of Hydrocenoses, Faculty of Fisheries and Protection of Waters, University of South Bohemia in České Budejovice, Zátiší 728/II, 389 25 Vodňany, Czech Republic*

Keywords
direct red 80
electrochemical oxidation
HPLC-HRMS
nontarget analysis

Abstract
Azo dyes are currently gaining more attention, especially as persistent contaminants. Due to the current issue of consumption and release of azo dyes into the environment it is necessary to constantly make progress in development of new advanced techniques that remove a wide range of organic micropollutants with high efficiency. The work is devoted to the application of electrochemical oxidation with boron-doped diamond electrodes for the elimination of selected azo dye, direct red 80. From the point of view of the safety profile of the treatment step, it is important to monitor the degradation products produced during the electrochemical oxidation. For this reasons, the second part of the work focuses on the identification of degradation products of direct red 80 using high-performance liquid chromatography and high-resolution mass spectrometry with nontarget approaches.

1. Introduction

Azo dyes are characterized by functional azo groups (−N=N−) and offer distinctive vivid colors. These synthetic dyes are widely used because of their low cost and high level of stability. According to statistics, the production of azo dyes reaches around 700,000 tons per year mainly due to their wide application potential in the cosmetic, paper, textile and plastic industries [1]. However, it has been estimated up to 60–70% of the total dye consumption is used to produce textile materials. Wastewater effluents from textile industrial plants are referred to primary polluting point with 200,000 tons of the colorants reaching the environment

every year. Azo dyes are classified as highly persistent compounds and well-known resistant to conventional chemical or biological treatment. In addition, the cleavage of the azo linkage results in the production of dangerous aromatic amine products. Therefore, recent studies have also investigated the toxicity of azo dyes and demonstrated carcinogenic, cytotoxic and mutagenic effects. For these reasons, it is crucial to invest research efforts in the development of new advanced processes that will be able to remove a wide range of contaminants including azo dyes [2, 3].

Currently, advanced oxidation processes are gaining a great attention as an effective technique for supplementary water treatment [4]. Advanced oxidation processes also include electrochemical oxidation using boron-doped diamond electrodes. By applying voltage to the electrode, organic compounds are oxidized either directly on the surface of the anode (direct oxidation) or contaminants are oxidized *in situ* by reactive radicals from the electrolyte solution (indirect oxidation). During electrochemical oxidation, the pollutants could be converted into more easily biodegradable compounds or their partial mineralization is monitored [5]. In comparison to other types of electrodes (Pt, RuO_2, IrO_2, etc.) boron-doped diamond electrodes has crucial advantages, described in more detail in work of Nidheesh et al. [6].

Recent studies have been showed the synthetic dyes are stable compounds but after environmental conditions are degraded and toxic by-products are formed. Therefore, the dye remediation process must be designed as an efficient and at the same time safe system for the entire environment and public health [2]. To assess the safety of the process it is necessary to identify emerging degradation and transformation products. However, the nontarget analysis requires the use of instrumentation with high-resolution. The combination of high-performance liquid chromatography with high-resolution mass spectrometry (HPLC-HRMS) represents a sensitive and selective analytical method suitable for the reliable identification of known and unknown compounds [7].

The work was focused on the study of direct red 80, where the main goals of the work were: (i) to evaluate the removal of direct red 80 by monitoring the discoloration of the solution (by UV-VIS) and (ii) to identify unknown degradation and transformation products by nontargeted approaches (by HPLC-HRMS).

2. Experimental

2.1 Reagents and chemicals

Electrochemical oxidation was performed using azo dye direct red 80 purchased from Synthesia (Cech Republic) with defined purity at the level 73.20%. Methanol (≥99.9%, LiChrosolv®) and acetonitrile (LC-MS Chromasolv®) were supplied from Merck (Germany). For preparation of mobile phases was used formic acid (≥98%) and acetic acid (≥99.88%) by Sigma-Aldrich.
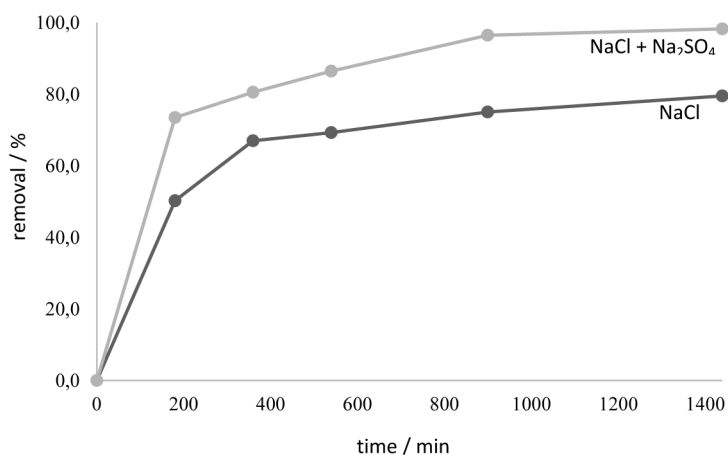
Fig. 1 Monitoring the removal efficiency of direct red 80. Composition of working electrolyte: NaCl (5 g/L), combination of NaCl + Na$_2$SO$_4$ (3.5 g/L and 1.5 g/L), c_0(direct red 80) = 100 mg/L, V(solution) = 0.5 L, U(cell) = 20 V.

2.2 Instrumentation

Electrochemical oxidation was performed by using porous boron doped diamond electrode deposited on porous ceramics. Degradation experiments were realized in deionized water with the addition of the direct red 80 (c_0 =100 mg/L) and also with salt addition (NaCl or in combination with Na$_2$SO$_4$). The evaluation of removal efficiency was based on monitoring absorbance value by the DR 6000 spectrophotometer (Hach Lange, Czech Republic) combined with LT 200 thermostat (Hach Lange, Czech Republic). The HPLC-ESI-IT-TOF-HRMS device had to be applied for identification of unknown degradation products of direct red 80 formed during electrochemical oxidation.

3. Results and discussion

3.1 Evaluation of removal efficiency using UV-VIS

All advanced oxidation processes are predominantly based on a sequence of oxidation-radical reactions. However, the formation of degradation products depends on the type of radical and the structure of the contaminant [8]. Degradation process using advanced oxidation processes is controlled by the rate of formation: ·OH, ·O$^-$, ·HO$_2$, ·O$_2^-$, H$_2$O$_2$, O$_2$, O$_3$, as well as competitive reactions. Other side reactions contribute to the degradation process of target compounds by ions originating from electrolytes or matrices. Typical examples are the presence of SO$_4^{2-}$ ions and the associated with formation of S$_2$O$_8^{2-}$ and Cl$^-$ with generation of Cl$_2$, HClO, HClO$_2$, HClO$_3$, HClO$_4$ [9].

According to Fig. 1, electrochemical oxidation is performed under mass transport control. In general the higher control of mass transport is, the lower

degradation efficiencies are achieved. For degradation treatment system is fundamental to produce the hydroxyl radicals and consume them respectively. The formation of strong oxidants in the solution is not limited by mass transport control, because of indirect oxidation can be performed in entire volume of system. However, if emerging DP is resistant to indirect oxidation the mass transport towards the electrode must be sufficient to reach oxidation by reactive OH radicals bound to the surface of the electrode [10]. In the first half of the degradation process, the azo dye direct red 80 is degraded at 69.3% in NaCl or 86.4% with combination of NaCl and Na_2SO_4, respectively. Figure 1 demonstrates the high elimination level (98.2%) of the selected azo dye has been obtained in the environment consisted of combination of NaCl and Na_2SO_4. The removal value is affected by (i) the composition of the working electrolyte and (ii) the formation of reactive particles species.

3.2 Identification of degradation products by HPLC-HRMS

For practical usage of advanced oxidation processes is crucial to monitor degradation efficiency, but should be also identified the emerging degradation products, which might cause undesirable secondary contamination in the environment. Special attention should be given to identification those compounds where it is expected the mutagenic and carcinogenic effects including azo dyes.

Optimization of mobile phase was performed using direct infusion of standard sample, where the level of ionization was monitored. After optimization process the mobile phase was consisted of 10mM acetic acid (pH = 3.31) and 100% acetonitrile. Than the fragmentation profile of direct red 80 was studied and characteristic fragmentation ions were identified. The HPLC conditions were chosen based on physical-chemical properties of direct red 80 characteristic for their presence of six $-SO_3^-$ function groups a strongly hydrophilic behavior. According to the properties of selected azo dye, it was used the chromatographic column Hypersil Gold aQ (50×2.1 mm, 3 μm) with gradient elution (linear trend from 0–100% B). Nontarget approach demands setting the HPLC-HRMS conditions are valid in general (to avoid the discrimination of some groups of compounds).

The nontargeted analysis uses data filtering based on a comparison with a blank. In the first step the chromatographic peaks are selected, which (i) are not in the blank, (ii) have a sufficient intensity value for MS/MS fragmentation to be performed. Then a list of potential candidates of degradation products is created and subjected to MS^n analysis. Based on mass spectra with high resolution in MS^1, it is possible to propose with higher certainty (mass accuracy) the assumed summary formula and according to fragmentation ion in MS^2 structural formula of the compound is proposed. During the degradation of direct red 80, the cleavage of the azo linkage results occurs. The compound breaks down into individual benzene nuclei, where oxidation of the $-NH_2$ group to $-NO_2$ is observed (Table 1).

Table 1
Potentially formed degradation products of direct red 80.

Compound	Proposed formula (ESI–)	m/z		MS^2 ions	Proposed structure
		Calculated	Measured		
DP$_1$	$C_6H_4SO_3N$	169.9912	169.9907	155.9895, 136.9992	
DP$_2$	$C_6H_3SO_5$	186.9701	186.9705	155.9885	
DP$_3$	$C_6H_3SO_4N_2$	198.9813	198.9809	177.9906, 119.023.	
DP$_4$	$C_6H_4SO_5N$	201.9810	201.9802	138.0209	
DP$_5$	$C_6H_3SO_5NCl$	235.9420	235.9417	154.9837	
DP$_6$	$C_6H_3SO_7N_2$	246.9661	246.9649	200.9719, 183.0046, 66.1390	

4. Conclusions

In the work, the effect of used salt on the removal efficiency of the selected azo dye direct red 80 was studied. The results showed the most effective elimination was achieved using a combination of sodium chloride and sodium sulfate with 3D boron-doped diamond electrodes on porous ceramics (98.2%). Using he combination of the HPLC-HRMS technique, it was possible to identify the unknown degradation products of electrochemical oxidation. Several degradation products were identified based on mass spectra with high resolution, exact masses of compounds and fragment ions in the MS^2 stage.

References

[1] Harichandaran G., Prasad S.: SonoFenton degradation of an azo dye, Direct Red. *Ultrasonics Sonochemistry* **29** (2016), 178–185.

[2] Nouren S., Bhatti N.H., Iqbal M., Bibi I., Kamal S., Sadaf S., Sultan M., Kausar A., Safa Y.: By-product identification and phytotoxicity of biodegraded Direct Yellow 4 dye. *Chemosphere* **169** (2017), 474–484.

[3] Tropp J., Ihde H.M., Crater R.E., Bell C.N., Bhatta R., Johnoson C.I., Bonizzoni M., Azoulay D.J.: Sensor array for the nanomolar detection of azo dyes in water. *ACS Sensors* **5** (2020), 1541–1547.

[4] https://run.unl.pt/bitstream/10362/118277/1/Fernandes_2021.pdf (accessed 1st July, 2022).

[5] Mackuľák T. et al.: *Environmentálne vedy – výskyt a možnosti degradácie polutantov.* Bratislava, FCHPT STU v Bratislave 2016. (In Slovak).

[6] Nidheesh V.P., Divyapriya G. Oturan N.,Trellu C., Oturan A.M.: Environmental application of boron-doped diamond electrodes: 1. Applications in water and wastewater treatment. *ChemElectroChem* **6** (2019), 2124–2142.

[7] Hollender J., Schymanski L.E., Singer P.H., Ferguson P.L.: Nontarget screening with high resolution mass spectrometry in the environment: ready to go? *Environmental Science & Technology* **51** (2017), 11505–11512.

[8] Miklos B.D., Remy C., Jekel M., Linden G.K., Drewes E.J., Hübner U.: Evaluation of advanced oxidation processes for water and wastewater treatment. *Water Research* **139** (2018), 118–131.

[9] Fang C., Megharaj M., Naidu R.: Electrochemical advanced oxidation processes (EAOP) to degrade per- and polyflluoroalkyl substances (PFASs). *Journal of Advanced Oxidation Technologies* **20** (2017), 20170014.

[10] Omninellis C.: *Electrochemistry for the Environment.* Springer, New York 2010.

Electrochemical determination of illicit drugs at 3D printed electrodes

Marta Choińska-Młynarczyk[a, b, *], Tomáš Navrátil[b]

[a] *Department of Analytical Chemistry, Faculty of Science, Charles University, Hlavova 8/2030, 128 43 Prague 2, Czech Republic* ✉ *marta.choinska@gmail.com*

[b] *J. Heyrovský Institute of Physical Chemistry of the Czech Academy of Sciences, Dolejškova 3, 182 23 Prague 8, Czech Republic*

Keywords

determination
lysergic acid
    diethylamide
psilocin
psilocybin
voltammetry

Abstract

Lysergic acid diethylamide, psilocin and psilocybin are neuroactive drugs. They can be use in experimental treatment in psychiatry, but also as illicit drugs for hallucinations and relaxation. These two types of use indicates that their monitoring in environment and in the body fluids is necessary. Electrochemistry offers fast, simple and easy methods for the determination with the possibility to use laboratory-manufactured electrodes from 3D printed materials. They offers many benefits, for example desired shape or diameter of the electrode, good developed signals, and low background currents. The advantage of this procedure is described in this contribution.

1. Introduction

Psilocin (4-hydroxy-*N,N*-dimethyltryptamine) and psilocybin (4-phospho-loxy-*N,N*-dimethyltryptamine) are two alkaloids which came from many fungus from the species *Psilocybe* (Fig. 1). Psilocybin is the natural alkaloid, which in the human body metabolizes to neuroactive psilocin. Their neuroactive properties indicate hallucinations and because of that mushrooms are widely used for religious purposes in some countries in Latin America. Moreover, they seems to be one of the most popular hallucinogenic drug in some subcultures [1–3].
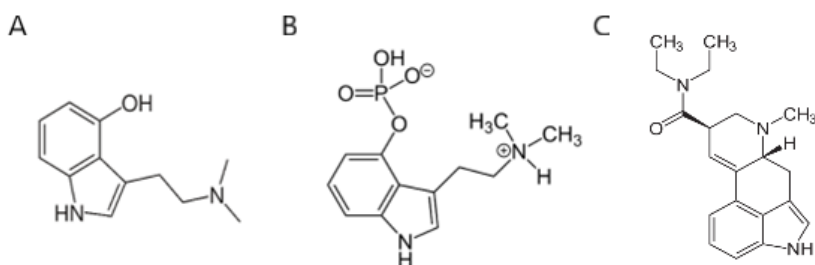

Fig. 1 Structures of (A) psilocin, (B) psilocybin, (C) lysergic acid diethylamide.

Neuroactive properties were also the subject of the interest of psychiatry. After rapid growth of the illegal use, they were not used for medical purposes for a long time. Recently their potential as drugs in psychiatry started to be one more time developed [3].

Lysergic acid diethylamide (LSD, Fig. 1) is a drug synthesized from lysergic acid, derived from ergotamine, the natural alkaloid from ergot. It was first derived in 1938 by Albert Hofmann for medical purposes. In 1943 its hallucinogenic effects were accidentally discovered. In 1940s and 1950s LSD was a subject of interest of psychiatrist and from 1960s its popularity as illicit drug has been growing [4–6]. It is worth to mention that LSD is one of the most potent drug, with only 100–150 μg (0.5–2.0 μg/kg) to observe hallucinations and in some cases even dose as small as 20-80 μg is enough to observe some influence [6].

In psychiatry LSD, psilocin and psilocybin were used for experimental treatment of depression, anxiety, changes in mood connected with terminal cancer, obsessive-compulsive disorder, post-traumatic stress disorder, and addiction. They may affect human mind positively and creates more self-confident and joyful feelings [3, 6–9].

Because of its positive treatment effects and also high possibility of abused or illicit use [10, 11], LSD, psilocin and psilocybin have to be monitored in the environment. During experimental treatments it is also necessary to monitor the amount of neuroactive compounds and its derivatives in human body (i.e., blood and urine). This caused that fast, easy, selective and sensitive methods of the determination are important for the medical, toxicological and ecological purposes.

Electrochemistry combined with the newly developed 3D printing electrodes and/or analytical platforms is very effective method of determination biologically active substances [12, 13]. It offers fast, inexpensive, selective and sensitive analysis. Moreover, 3D printing gives the opportunity to achieve exactly desired shape or diameter of the electrode or designed platform [14, 15]. Because of these advantages we decided to use voltammetric methods with 3D printed electrodes for the determination of LSD, psilocin and psilocybin.

2. Experimental

2.1 Reagents and chemicals

The following biologically active compounds were selected for our experiments: psilocin, psilocybin, and lysergic acid diethylamide (every of them from Lipomed, Switzerland). Stock solution of psilocin was prepared by dissolving it in methanol (Lach-Ner, Czech Republic) and the solution of psilocybin was prepared by dissolving it in deionized water. Stock solution of LSD was prepared by its dissolution in 0.1 mol dm^{-3} lithium perchlorate (Sigma Aldrich, USA).

Britton-Robinson Buffer from pH = 3 to pH = 12 was prepared from 0.04 mol dm^{-3} boric acid, 0.04 mol dm^{-3} phosphoric acid, 0.04 mol dm^{-3} acetic acid

Table 1
Optimized parameters for the differential pulse voltammetric determination of psilocin, psilocybin and lysergic acid diethylamide.

Parameter	Analyte		
	Psilocin	Psilocybin	Lysergic acid diethylamide
pH	3	3	7
E_{acc}/mV	–500	400	100
t_{acc}/s	60	60	300
v/mV s^{-1}	20	20	20

and 0.2 mol dm^{-3} sodium hydroxide (every of them Penta, Czech Republic). For all described measurements deionized water from Milli-Q-Gradient (Millipore, Czech Republic), conductivity <0.05 μS cm^{-1}, was used.

2.2 Instrumentation

Voltammetric measurements were performed using Eco-Tribo Polarograph (Polaro-Sensors, Czech Republic), controlled by the software MultiElChem 3.3 for Windows 10 (J. Heyrovský Institute of Physical Chemistry of the Czech Academy of Sciences, Czech Republic). Results were recorded by 3D printed carbon fiber PLA working electrode (CF-PLAE, laboratory-made). For manufacturing of 3D printed electrode, the carbon PLA filament ProtoPasta (ProtoPlant, USA) was used. Ag|AgCl(3 mol dm^{-3} KCl) was used as the reference and platinum wire as the auxiliary electrode (both Elektrochemické detektory, Czech Republic). Buffer pH was measured with pH-meter Jenway 3505 (Bibby Scientific Limited, UK).

3. Results and discussion

Our research started with the optimization of the measurements procedure with cyclic and differential pulse voltammetry. Different buffers, scan rates, accumulation potentials and times were tested to achieve the best developed signals. Before each series of three experiments, electrode wad polished on sand paper 400Q, ten times cyclic voltammetry (E_{ini} = –1500 mV, E_{fin} = +1500 mV, v = 100 mV s^{-1}. Optimal parameters are summarized in Table 1.

After the parameters optimization psilocin and psilocybin were determined by DPV method at 3D printed electrode in the wide range of the concentration (from 10^{-7} to 10^{-5} mol dm^{-3}). The results are shown at Fig. 2.

We observe that psilocin signal (500 mV) was much better developed and almost two times higher than the psilocybin signal (800 mV) in the same concentration of the compound. We also may see at Fig. 2A that even in the pure psilocybin solution small signal of psilocin was achieved around 500 mV. It may suggest that during dissolution process and during the electrochemical
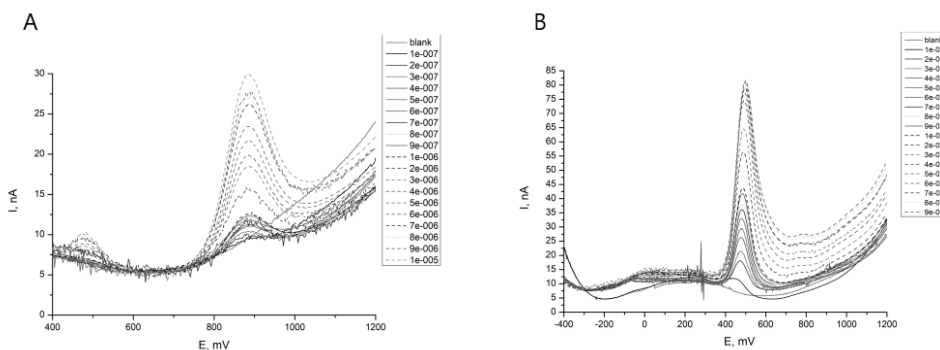
Fig. 2 Differential pulse voltammograms of (A) psilocybin, and (B) psilocin in the concentration from 10^{-7} to 10^{-5} mol dm^{-3}. Psilocybin measurement parameters: pH = 3, E_{acc} = 400 mV, t_{acc} = 60 s, v = 20 mV s^{-1}. Psilocin measurement parameters: pH = 3, E_{acc} = –500 mV, t_{acc} = 60 s, v = 20 mV s^{-1}.

measurement some part of psilocybin was transferred to psilocin. It also shows that in the next part of the experiment simultaneous determination of these two compounds will be possible.

Cyclic voltammetry with different scan rates (from 10 mV s^{-1} to the 1280 mV s^{-1}) was used for the elimination voltammetry which may give us more information about the reaction mechanism. Data analysis is in progress.

After optimization of the parameters LSD determination and data analysis is in progress.

4. Conclusions

First and finished part of our research shows that 3D printed electrodes are useful tools for the electrochemical determination of illicit drugs. They offer very good signals which may be easily increased with the further modification of the surface. We also proved that we can simultaneously observe signals of two alkaloids. Further research and data analysis will develop the next information about mechanism of the reaction and possibilities of voltammetry use for medical, toxicological or environmental purposes.

Acknowledgments

References

[1]   Geiger H.A., Wurst M.G., Daniels R.N.: DARK Classics in chemical neuroscience: Psilocybin. *ACS Chemical Neuroscience* **9** (2018), 2438–2447.

[2]   Fradkin D.: Psilocybin: A brief overview for psychiatric mental health nurse practitioners. *Perspectives in Psychiatric Care* (2021), DOI: 10.1111/ppc.12888

[3]   Zeiss R., Gahr M., Graf H.: Rediscovering psilocybin as an antidepressive, treatment strategy. *Pharmaceuticals* **14** (2021), 985.

[4]   Brandt S.D., Kavanagh P.V., Westphal F., Stratford A., Odland A.U., Klein A.K., Dowling G., Dempster N.M., Wallach J., Passie T., Halberstadt A.L.: Return of the lysergamides. Part VI: Analytical and behavioural characterization of 1-cyclopropanoyl-*d*-lysergic acid diethyl-amide (1CP-LSD). *Drug Testing and Analysis* **12** (2020), 812–826.

[5]   Grumann C., Henkel K., Brandt S.D., Stratford A., Passie T., Auwarter V.: Pharmacokinetics and subjective effects of 1P-LSD in humans after oral and intravenous administration. *Drug Testing and Analysis* **12** (2020), 1144–1153.

[6]   Fuentes J.J., Fonseca F., Elices M., Farr M., Torrens M.: Therapeutic use of LSD in psychiatry: A systematic review of randomized-controlled clinical trials. *Frontiers in Psychiatry* **10** (2019), 943.

[7]   Heuschkel K., Kuypers K.P.C.: Depression, mindfulness, and psilocybin: Possible complementary effects of mindfulness meditation and psilocybin in the treatment of depression. A review. *Frontiers in Psychiatry* **11** (2020), 224.

[8]   Johnson M.W., Griffiths R.R.: Potential therapeutic effects of psilocybin. *Neurotherapeutics* **14** (2017), 734–740.

[9]   Bogenschutz M.P., Johnson M.W.: Classic hallucinogens in the treatment of addictions. *Progress in Neuro-Psychopharmacology and Biological Psychiatry* **64** (2016), 250–258.

[10]   Johnson M.W., Griffiths R.R., Hendricks P.S., Henningfield J.E.: The abuse potential of medical psilocybin according to the 8 factors of the Controlled Substances Act. *Neuropharmacology* **142** (2018), 143–166.

[11]   Yockey R.A., Vidourek R.A., King K.A.: Trends in LSD use among US adults: 2015–2018. *Drug and Alcohol Dependence* **212** (2020), 108071.

[12]   Porto, L., Silva, D., de Oliveira, A., Pereira, A., Borges, K.: Carbon nanomaterials: synthesis and applications to development of electrochemical sensors in determination of drugs and compounds of clinical interest. *Reviews in Analytical Chemistry* **38** (2019), 20190017.

[13]   Rocha R.G., Ribeiro J.S., Santana M.H.P, Richter E.M., Muñoz R.A.A.: 3D-printing for forensic chemistry: voltammetric determination of cocaine on additively manufactured graphene-polylactic acid electrodes. *Analytical Methods* **13** (2021), 1788.

[14]   João A.F., Rocha R.G., Matias T.A., Richter E.M., Petruci J.F.S., Muñoz R.A.A.: 3D-printing in forensic electrochemistry: Atropine determination in beverages using an additively manufactured graphene-polylactic acid electrode. *Microchemical Journal* **167** (2021), 106324.

[15]   Choińska M., Hrdlička V., Dejmková H., Fischer J., Míka L., Vaněčková E., Kolivoška V., Navrátil T.: Applicability of selected 3D printing materials in electrochemistry. *Biosensors* **12** (2022), 308.

Author Index

Keyword Index

knihovnicka.cz